

Impacts of Psychrophilic Conditions on Anaerobic Membrane Bioreactors
Treating Municipal Wastewater

by

Linda Li

A thesis

presented to the University of Waterloo

in fulfillment of the

thesis requirement for the degree of

Master of Applied Science

in

Civil Engineering

Waterloo, Ontario, Canada, 2019

© Linda Li 2019

Author's Declaration

I hereby declare that I am the sole author of this thesis. This is a true copy of the thesis, including any required final revisions, as accepted by my examiners. I understand that my thesis may be made electronically available to the public.

Abstract

In an anaerobic membrane bioreactor (AnMBR) system, the conversion of biogas from organics is accomplished through anaerobic digestion. Temperature has a significant impact on the metabolic activities of the biomass present in these systems, as well as affecting gas-transfer rates and other physical processes. Historically, AnMBRs have typically been operated at mesophilic or thermophilic temperatures and there are few reports of operation at psychrophilic temperatures. The motivation for this project was to evaluate the impact of psychrophilic temperatures on AnMBRs and to evaluate measures to improve AnMBR performance at these temperatures.

Three 5 L AnMBRs that incorporated submerged ZeeWeed® hollow fibre PVDF membranes with a nominal pore size of 0.04 μm and a nominal membrane surface area of 0.047 m^2 were employed. The AnMBRs were operated at a solids retention time (SRT) of 30 days and a hydraulic retention time (HRT) of 0.4 days. At the start of the study, the AnMBRs were inoculated with primary digester effluent obtained from the Galt Wastewater Treatment Plant. After inoculation, the daily feed into the AnMBRs was pumped out of a wet well receiving municipal sewage from a City of Waterloo sanitary sewer line at the University of Waterloo.

Throughout the study, a daily volume of 10.13 L of wastewater was fed to each AnMBR, 0.130 L of Waste Sludge was manually wasted, and 10 L of permeate was generated. The AnMBRs were operated in a relaxed mode with 8 minutes of permeation followed by 2 minutes of relaxation and were operated at a constant flux while Transmembrane Pressure (TMP) was monitored. Gas sparging was provided to the AnMBRs to reduce membrane fouling.

This study was conducted in three phases. During the initial phase of operation, the AnMBRs were operated at 24°C, 15°C and 10°C respectively. TCOD, SCOD, TSS, VSS, VFA, biogas production, pH and TMP were regularly monitored to characterize the physical and biological performance of the AnMBRs. Compared to operation at 24°C, operation at 10°C resulted in decreased permeate quality, lower biogas production, and unconsumed volatile fatty acids. There was no significant difference in performance of the AnMBR operated at 24°C and 15°C.

During the second phase, one AnMBR was maintained at 24°C while two AnMBRs were operated at 10°C. The psychrophilic AnMBRs both exhibited decreased permeate quality, lowered biogas production, and unconsumed volatile fatty acids. Moreover, TMP spikes were observed in the psychrophilic AnMBRs, suggesting increased membrane fouling due to lowered temperatures.

In the final phase of the study, Powdered Activated Carbon (PAC) was added to one of the AnMBRs operated at 10°C to achieve a concentration of 2 g/L as a biofilm carrier. After 90 days of operation, the previously accumulated VFAs in this AnMBR declined in concentration, while the VFAs in the AnMBR without PAC were consistently elevated. In contrast to Phase II, the psychrophilic AnMBR with PAC showed no significant TMP spikes in a five day period, suggesting improved permeability. However, methane production was not increased due to the addition of PAC in the psychrophilic AnMBR.

Through completing the study a few important contributions to the operation of AnMBRs in cold regions can be drawn. In terms of the biological performance of AnMBRs, compared to the 24°C operation, operation at 10°C was observed to have decreased permeate quality, lower biogas production, and unconsumed VFAs. However, there was no significant difference in the performances of the 24°C and 15°C AnMBRs. VFA accumulation in the psychrophilic AnMBR with PAC addition decreased. VFAs in the psychrophilic AnMBR without PAC were consistently elevated. In terms of the physical performance of each AnMBR, TMP spikes were observed in the psychrophilic AnMBRs, suggesting increased membrane fouling due to lowered temperatures. TMP results suggest that improved permeability can be achieved through PAC addition.

Acknowledgements

Firstly of all, I would like to express my sincere gratitude to my advisor, Dr. Wayne Parker, for the continuous support throughout my graduate study. His guidance, patience, and immense knowledge in the wastewater treatment field helped me complete this degree.

Besides my advisor, I would like to thank Mark Merlau and Mark Sobon for their unwavering support and assistance with troubleshooting lab equipment and conducting analyses. Without their precious support, it would not be possible to conduct this research. I am also very grateful to our Project Manager Thomas Sullivan for his words of encouragement and guidance.

A special thanks goes to Mihail Filippov for teaching me the various lab analysis techniques and helping me start up the operations of my bioreactors. I would also like to acknowledge the help from coop students Ana Damasceno, Gary Voorthuyzen, Cameron Adams, and Stella Garcia for their help with the maintenance of my bioreactors.

Last but not least, I am deeply grateful to my family and friends for their unconditional love and support. Words cannot express how fortunate I feel to have my wonderful parents, Jun Li and Jing Wang, who were always actively participating in conversations with me about my research and being there for me through difficult times. My thesis stands as a testament to your unconditional love and encouragement.

Table of Contents

Author's Declaration	ii
Abstract	iii
Acknowledgements	v
List of Figures	viii
Chapter 1: Introduction	1
1.1 Motivation	1
1.2 Objectives	2
1.3 Thesis Structure	3
Chapter 2: Literature Review	4
2.1 Anaerobic Membrane Bioreactors (AnMBR)	4
2.2 Biological Performance of AnMBR	7
2.3 Membrane Fouling Challenge	9
2.4 Effect of Temperature on Membrane Fouling	10
2.5 Fouling Control Mechanism by Biofilm Carriers	12
2.6 Future Research Needs	15
Chapter 3: Materials and Methods	16
3.1 AnMBR Configuration	16
3.2 Operational Conditions	18
3.3 Inoculum and Feed Characterization	19
3.4 Experimental Design	21
3.5 Sampling Protocol	23
3.6 Sample Analysis	24
3.6.1 Total COD	24
3.6.2 Soluble COD	25
3.6.3 Suspended Solids	25
3.6.4 Volatile Fatty Acids	25
3.6.5 Sulfate	26
3.6.6 pH	26

Chapter 4: Results and Discussion.....	27
4.1 Overall Biological Performance.....	27
4.2 Phase 1 AnMBR Performance.....	32
4.3 Phase 2 AnMBR Performance.....	40
4.4 Phase 3 AnMBR Performance.....	48
Chapter 5: Conclusions and Recommendations.....	66
5.1 Conclusions.....	66
5.2 Recommendations.....	67
References.....	68
Appendix A.....	71
Appendix B.....	81
Appendix C.....	86

List of Figures

Figure 1: Schematic Diagram of the Lab Scale AnMBRs used in the study	16
Figure 2: Actual set up of the psychrophilic AnMBRs	18
Figure 3 Influent vs Effluent COD Concentrations throughout the Study.....	28
Figure 4 Influent vs Accumulated VFA throughout the Study	29
Figure 5 Influent COD vs CH ₄ Production throughout the Study.....	31
Figure 6 ANOVA Summary on Phase 1 Average COD Removal Efficiencies.....	33
Figure 7 Tukey Test Summary on Phase 1 Average COD Removal Efficiencies	34
Figure 8 Phase 1 COD Mass Balance for the 24°C MBR	36
Figure 9 Phase 1 Influent vs Effluent VFA-COD	38
Figure 10 Phase 1 Methane Production Results	39
Figure 11 ANOVA Summary on Phase 2 Average COD Removal Efficiencies	41
Figure 12 Tukey Test Summary on Phase 2 Average COD Removal Efficiencies	42
Figure 13 Phase 2 Steady State COD Mass Balance for the 24°C MBR.....	44
Figure 14 Phase 2 Influent vs Effluent VFA-COD	46
Figure 15 Phase 2 Methane Production Results.....	47
Figure 16 Phase 3 Effluent COD vs Influent COD Results	49
Figure 17 ANOVA Summary on Phase 3 Average COD Removal Efficiencies	50
Figure 18 Tukey Test Summary on Phase 3 Average COD Removal Efficiencies	51
Figure 19 Phase 3 Steady State COD Mass Balance for the 24°C MBR.....	53
Figure 20 Phase 3 Influent vs Effluent VFA-COD	55
Figure 21 Phase 3 Methane Production Results	57
Figure 22 TMP Results from the 24°C, 15°C, and 10°C AnMBRs during Phase 1.....	61
Figure 23 TMP Results from the 10°C AnMBRs during Phase 3.....	63

Chapter 1: Introduction

1.1 Motivation

Environmental sustainability has become one of the most important factors when designing a wastewater treatment system. In the field of municipal wastewater treatment, anaerobic membrane bioreactor (AnMBR) systems are emerging as a promising technology. AnMBR systems integrate membrane filtration into the anaerobic biological wastewater treatment process, producing a high quality permeate in a single stage. Compared to conventional aerobic treatment processes that require high energy input and generate large quantities of sludge, AnMBR systems have many advantages. While producing only a fraction of the sludge generated by aerobic systems, AnMBRs can achieve methane-rich biogas production through anaerobic conversion of the organics in municipal wastewater (Smith et al., 2014). A number of studies assessing AnMBR performance in municipal wastewater treatment have been published. For example, Smith et al. (2014) operated a bench-scale AnMBR equipped with submerged flat-sheet microfiltration membranes was operated at psychrophilic temperature (15°C) treating simulated and actual domestic wastewater (DWW). Martinez-Sosa et al. (2011) operated a pilot scale anaerobic submerged membrane bioreactor for municipal wastewater treatment for 100 days. Baek et al. (2010) operated a completely mixed anaerobic bioreactor at 32°C and assessed the impacts of HRT on AnMBR permeate quality. Several other studies similarly evaluated the correlations between various parameters such as HRT, SRT, and temperature with AnMBR performance (Ho and Sung, 2009; Lew et al., 2009; Salazar-Pelaez et al., 2011).

AnMBRs can provide many benefits that aerobic membrane bioreactors (AeMBRs) provide and do so with less energy demand. AeMBRs have been shown effective in the treatment of both

high and low strength wastewater as membrane costs have decreased dramatically (Smith et al., 2014). AeMBRs provide superior effluent quality compared to conventional aerobic treatment and reduce the footprint required to construct and operate the treatment system. Overall the membrane industry in wastewater treatment is predicted to have a mean growth rate of approximately 12% from 2000 to 2013 (Smith et al., 2014).

While the application of AnMBRs to municipal wastewaters is attractive, their ability to operate at psychrophilic temperatures has proved challenging (Lettinga et al., 2001; Martin et al., 2011). In Canada where temperatures are low, operation of AnMBRs at mesophilic temperatures is likely not feasible for a significant portion of the year and hence it is important to characterize AnMBR operation at lower temperatures that those that have been reported in most of the published literature. Appropriate modifications to the treatment system, such as reactor configuration and hydraulic loading conditions, could then be designed. This study aims to contribute to this area of research.

1.2 Objectives

The objectives of this research were to:

- Evaluate the biological performance of AnMBRs under psychrophilic conditions
- Investigate the fouling behavior of the membranes in AnMBRs under psychrophilic conditions
- Explore mitigation strategies to improve AnMBR performance at psychrophilic temperatures

1.3 Thesis Structure

This thesis is divided into five sections. Section 1 provides a brief explanation of the problem under investigation and the motivation behind the research. Chapter 2 summarizes relevant research on operating AnMBRs at low temperatures and membrane fouling management in both aerobic and anaerobic MBRs. Chapter 3 documents the methodology employed in this study, which includes the configuration, operation, and maintenance of the AnMBRs, as well as analysis procedures followed throughout the study. Chapter 4 presents the results obtained from the study, in terms of both biological and physical performance evaluations of the AnMBRs. Chapter 5 provides significant conclusions from the study as well as recommendations for further research.

Chapter 2: Literature Review

In this chapter, a summary of existing research in the area of AnMBR operation is provided. Section 2.1 provides an overview of the AnMBR operation in wastewater treatment and parameters impacting performance of AnMBRs. Section 2.2 discusses the studies already done to assess the biological performance of AnMBR. Section 2.3 focuses on the fouling mechanisms in AnMBRs and fouling control measures employed by various researchers. Section 2.4 discusses the impacts of temperatures on AnMBR performance and the studies already conducted to assess AnMBR performance at psychrophilic temperatures. Section 2.5 discusses the role of biofilm carriers in the control of membrane fouling. Lastly, Section 2.6 outlines suggested future research needs in the area of AnMBR operation at psychrophilic temperatures.

2.1 Anaerobic Membrane Bioreactors (AnMBR)

Anaerobic digestion is a multistep biochemical process that consists of four fundamental steps, which include hydrolysis, acidogenesis, acetogenesis, and methanogenesis. Biomass is normally comprised of unsuable large organic polymers including proteins, fats and carbohydrates (Biarnes, M., 2014). Hydrolysis is the essential first step that breaks down these large polymers and turns them into smaller molecules such as amino acids, fatty acids, and simple sugars. Following hydrolysis, molecules that are still too large must be further broken down in the process of acidogenesis. As the name suggests, acidogenesis involves acidogenic bacteria that create an acidic environment while producing shorter volatile fatty acids, ammonia, and carbon dioxide. Organic matter that is still too large for methane production next undergoes the process

of acetogenesis, in which acetogens break biomass down to the point where it can be utilized by methanogens to create methane (Biarnes, M., 2014).

Only under favorable environmental conditions will these anaerobic microorganisms survive and reproduce. Temperature has a significant impact on the metabolic activities of these microorganisms as well as a profound effect on gas-transfer rates and settling characteristics of the biomass (Metcalf and Eddy, 2003). There exist three temperature ranges in which various types of microorganisms may survive. Psychrophilic conditions refer to 10-30 °C; mesophilic conditions refer to 20-50 °C; and thermophilic conditions are from 35 to 75°C (Metcalf and Eddy, 2003). To ensure optimal microbial activity, AnMBRs are typically operated at mesophilic or thermophilic temperatures (Martinez-Sosa et al., 2012). At psychrophilic temperatures, the conversion of biomass slows down due to the decreased rate of hydrolysis. In addition to the biological factor, membrane performance worsens because of the drop in biosolid settling rate caused by an increased viscosity. Also, solubility of gaseous compounds increases as temperature drops to below 20°C, which means that dissolved concentrations of methane, hydrogen sulfide and hydrogen will be higher in the treated effluent (Lettinga et al., 2001).

A number of studies assessing AnMBR performance at psychrophilic temperatures have been published. Martinez-Sosa et al. (2011) operated a pilot scale anaerobic submerged membrane bioreactor for municipal wastewater treatment for 100 days. During the first 69 days, the reactor was operated under mesophilic temperature conditions. Afterwards, the temperature was gradually reduced to 20°C. An increase in the fouling rate was observed at 20°C. The COD removal efficiency was close to 90% under both temperature ranges. The final effluent COD was

less than 20 mg/L at volumetric organic loading rate of 0.5 to 12.5 kg/m³·day. Chu et al. (2005) evaluated the performance of an expanded granular sludge bed (EGSB) reactor coupled with hollow fibre membrane filtration for treating domestic wastewater in the range 11–25 °C. With temperatures above 15 °C, the system was capable of removing 85–96% of total COD. At 11 °C, the total COD removal was observed to be 76% and 81%, at an HRT of 3.5 and 5.7 h, respectively. Applying a higher upflow velocity contributed to better effluent removal efficiency and a higher membrane permeability. The results of tests showed that cake layer resistance was the major resistance. More extracellular polymer substances (EPS) tended to be accumulated on the membrane surface than in the granules since its content was higher on the membrane surface than in the granules.

In a study conducted by Smith et al. (2013), a bench-scale AnMBR equipped with submerged flat-sheet microfiltration membranes was operated at 15°C for treating simulated and actual domestic wastewater. An average removal efficiency of $92 \pm 5\%$ COD was achieved, which corresponds to an average permeate COD of 36 ± 21 mg/L in simulated DWW and $69 \pm 10\%$ in the actual DWW treatment. In another study by Smith et al. (2015), a simulated domestic wastewater was treated using an AnMBR at psychrophilic temperatures of 15, 12, 9, 6, and 3°C. A COD removal of greater than 95% was achieved when the AnMBR was operated at 6°C. However, the COD removal was observed to be reduced to 86% at 3°C. It was hypothesized that as temperature decreased, suspended biomass activity reduced resulting in an increase in soluble COD in the bioreactor. The high removal efficiency of COD at 6°C was attributed to viable microbial activity in the membrane biofilm. The performance improvement associated with using a biofilm carrier inside an AnMBR will be discussed later on in this chapter.

2.2 Biological Performance of AnMBR

There are several parameters that have been shown to impact the biological performance of an AnMBR, including HRT, SRT, operating temperature, influent COD, and biomass retention measures.

Several researchers have investigated the trade-off between controlling HRT and SRT for membrane fouling mitigation and achieving treatment performance requirements. These two parameters are key in optimising the performance of an AnMBR. Low HRTs mean smaller reactors and lower costs, while long SRTs enable very low sludge yields for disposal (Stuckey, 2010). Studies have found that a low HRT is desirable to reduce AnMBR size and the overall footprint of operation, in addition to achieving high COD removals. In a study conducted by Hu and Stuckey (2006), a submerged AnMBR with 0.4 μm hollow fiber membrane was operated at HRTs of 48 hr, 24 hr, 12 hr, 6 hr, and 3 hr. The SRT throughout the study was infinite and the operating temperature was consistently 35°C. At an HRT as low as 3 hr, the total COD removal achieved was 90%. The same AnMBR was able to remove 95% of total COD when operated at an HRT of 48 hrs. In another study conducted by Baek and Pagilla (2006), a completely mixed AnMBR with a 0.1 μm PVDF external tubular membrane operated at 32°C had shown a 68% total COD removal at an HRT of 12hr and a 58% total COD removal at an HRT of 48 hr. The SRT in Baek and Pagilla's study was also infinite. Both of these two studies suggest that when HRT is lowered, to achieve a high COD removal, a high SRT may be required. This could be attributed to the fact that in AnMBRs with high SRT, or even infinite SRT, biomass retention increases since no sludge is wasted. At long SRTs the sludge will be minimal and very non-biodegradable, however. A disadvantage of running AnMBRs are long SRTs is the fact that

Biomass Associated Products (BAPs), which form part of SMPs in the digester, tend to increase with SRTs, and this tends to increase effluent COD (Stuckey, 2010).

One step above evaluating the effect of SRT vs HRT is introducing operating temperature into the variation of SRT and HRT. Temperature has a significant impact on the metabolic activities of the biomass present in AnMBRs and studies have evaluated how SRT and HRT in combination with a low operating temperature could affect AnMBR performance. At a high SRT, increasing the HRT could also improve the AnMBR performance when temperature is reduced. In the study conducted by Chu et al. (2005), the performance of an expanded granular sludge bed (EGSB) reactor coupled with hollow fibre membrane filtration for treating domestic wastewater was monitored during 7-month period in the range 11 – 25 °C, and at the HRT of 3.5 to 5.7 hr. The SRT in this study was kept at 145 days. With temperatures above 15 °C, the system was capable of removing 85–96% of total COD and 83–94% of total organic carbon (TOC). At 11 °C, increasing HRT from 3.5 to 5.7 h, the total COD removal was increased from 76 to 81%. In another study conducted by Wen et al. (1999), a UASB with submerged membrane was operated at 12 – 25 °C. The SRT of the study was kept at 150 d and two different HRTs were employed. At an HRT as low as 4 hrs, a total COD removal of 97% was possible even at temperatures down to 13 °C, with almost complete methane recovery in the gas phase. This study has shown extremely good total COD removal efficiencies compared to the other AnMBRs operated at low temperatures.

2.3 Membrane Fouling Challenge

Membrane fouling has been a major challenge in the operation of AnMBRs. There has been extensive research done on fouling mechanisms and in almost all membrane processes fouling is normally caused by the accumulation of inorganic and organic foulants on the membrane surface or in membrane pores. Membrane fouling increases trans-membrane pressure during the liquid – solid physical separation process, and thereby reducing the productivity of the AnMBR. The fouling process normally includes pore blocking and solute aggregation that leads to cake formation on the membrane surface (Li & Chen, 2010). The primary foulants in AnMBR systems include soluble microbial products (SMP), colloidal particles from the feed and cell lysis, inorganic precipitates, and extracellular polymeric substances (EPS) (Smith, 2014). These foulant formations are influenced by a range of parameters such as the composition of the biological system, membrane type, hydrodynamic conditions, reactor operating conditions, process performance targets and the chemical system (Stuckey, 2010).

SMPs are critical in membrane fouling. In AnMBRs with high SRTs the production of SMPs from cell lysis is high, and much of the soluble COD in the reactor is SMPs (Stuckey, 2010).

There has been very little research on fouling mechanisms in submerged AnMBRs. Akram and Stuckey (2008) investigated the start-up of a submerged AnMBR for the treatment of a sucrose-meat extract based medium strength wastewater. At an HRT of 30 hours, the AnMBR achieved more than 90% chemical oxygen demand (COD) removal. The study found that the low flux (2 LMH) during high strength treatment was attributed to fine colloids, and high amounts of SMP.

In addition to SMPs and colloidal particles, research has also shown that inorganic precipitates contribute to membrane fouling. The role of inorganic fouling in AnMBRs depends on the

chemical composition of the wastewater feed. Some common precipitates include struvite, phosphate and calcium salts. In anaerobic systems where the concentrations of both ammonia and carbonate ions are higher than aerobic systems, precipitation with these ions is more likely (Stuckey, 2010).

A range of key parameters influence the fouling rate inside the AnMBR, including temperature, hydrodynamics, HRT, SRT and organic loading rate. The next section focuses on the research done in the area of the impact of temperature on membrane fouling, as it is the primary interest of this study.

2.4 Effect of Temperature on Membrane Fouling

Temperature variations in an AnMBR can be caused by seasonal fluctuations, frequent temperature transits of wastewater streams, or failure to control temperatures due to unexpected heating and cooling issues. It is important to understand the effects of temperature on the treatment system performance in case of unexpected variations. One major effect that temperature has been found to have on AnMBR performance was membrane fouling. The effect of operating temperature on membrane fouling in AnMBRs has been studied and reported by several researchers.

One research study looked at the impact of temperature at thermophilic and mesophilic temperatures. Lin et al. (2009) operated two submerged AnMBRs at thermophilic and mesophilic temperatures for a period of 3.5 months. The filtration resistance observed in the thermophilic AnMBR was about 5-10 times higher than that of the mesophilic system when operated under similar hydrodynamic conditions. Comparison of sludge properties and cake layer structure from

the two systems was made to find more SMP and biopolymer clusters produced in the thermophilic AnMBR. A series of analyses showed that the cake layer formed in the thermophilic AnMBR contained higher levels of both organic and inorganic foulants, smaller particle sizes, and a denser and more compact sludge cake structure.

Other studies evaluated the impact of temperature at psychrophilic conditions. Ma et al., (2013) aimed to investigate the effect of temperature variation on membrane fouling and microbial community in a membrane bioreactor. Trans-membrane pressure (TMP) spikes were observed under low-temperature operations, indicating membrane fouling. The results indicated that extracellular polymer substances (EPS) and soluble microbial products (SMPs) increased due to decreasing temperature, which triggered membrane fouling.

Wang et al. (2010) also investigated the effect of temperature on membrane fouling. The study observed deterioration in the settling and dewaterability of mixed liquor under low-temperature operations. The deterioration in settling and dewaterability could be an indicator of increased levels of EPS in sludge, which are suspected to lead to increased membrane fouling.

More AnMBR studies have pointed to EPS as a major contributor to direct membrane fouling at psychrophilic temperatures. Chu et al. (2005) operated an EGSB coupled with microfiltration initially at 25°C and subsequently operated at 20, 15, and 11°C. Chu discovered that the specific EPS deposited on the membrane surface was twice that found in the granular sludge. The discrepancy between biomass and cake layer EPS composition suggests that soluble or colloidal compounds are responsible for the increase in membrane resistance in AnMBRs.

2.5 Fouling Control Mechanism by Biofilm Carriers

Several mechanisms have been applied to mitigate membrane fouling in AnMBRs, such as backflushing, membrane relaxation, biogas sparging, and chemical cleaning.

Backflushing has been found to successfully remove reversible fouling caused by colloidal particles that clog the pores of the membrane. It is the process of physically cleaning the membrane without chemicals by reversing permeate through the membrane. In the study where Chu et al. (2005) operated an EGSB with submerged membrane, backflushing and relaxation were both employed as fouling control measures. Periodic chemical cleaning with 0.03% NaOCl was also used. In a different study, Ho and Sung (2010) operated two laboratory-scale AnMBRs in parallel at 25 and 15 °C. Throughout the operation the membrane flux was fixed to 5 MLH with TMP of 6.9–55.2 kPa. The membrane flux was maintained at 5 LMH. Backflushing using permeate was carried out to restore flux at every 4–6 days and no chemical cleaning was attempted.

Biogas sparging has been developed as an in-situ cleaning mechanism to control membrane fouling. Air is taken from the headspace inside the bioreactor and injected back into the mixed liquor just by the surface of the membrane to scour the particles and remove other deposited materials on the cake layer. Several studies have employed biogas sparging as a fouling control mechanism. Martinez-Sosa et al. (2011) employed gas sparging as a fouling control mechanism during the operation of a pilot scale submerged AnMBR with an external filtration unit. In addition to gas sparging, shear was created by circulating sludge. The experiment was conducted for 100 days and the reactor was operated under mesophilic temperature conditions during the

first 69 days. A slow and linear increase in the filtration resistance was observed under critical flux conditions at 7 LMH at 35 °C. The temperature was gradually reduced to 20 °C after the mesophilic phase, and an increase in the fouling was observed at 20 °C. Using biogas sparging and backflushing concurrently has been observed to be more effective than either control method alone in aerobic MBRs (Smith et al., 2014).

Chemical cleaning has also been a widely accepted mechanism to control membrane fouling. Commonly used chemicals include sodium hypochlorite, citric acid, sodium hydroxide, and hydrogen peroxide. Sodium hypochlorite has been mainly used for organic foulants while citric acid for inorganic foulants. Research has also found that a low concentration of chemical agents can be added to backflushing permeate stream to achieve chemically enhanced backflush (Hai et al., 2013).

Another mechanism to control fouling that has received attention in recent years is through the adsorption of the foulants using activated carbon, cationic polymers, biopolymers, or metal salts. Park et al. (1999) was the first reported research that evaluated the effect of powdered activated carbon (PAC) addition on the performance of an AnMBR. The performance was measured in terms of membrane filterability and treatability through a series of batch and continuous microfiltration experiments. In both operational modes, the flux was improved with PAC addition. When a higher shear rate and/or a higher PAC dose were applied, both the fouling and cake layer resistances decreased continuously with increasing the PAC dose up to 5 g/L. Aside from adsorbing the dissolved organics and colloidal particles in the mixed liquor, PAC was believed to have a scouring effect for removing the deposited biomass cake from the membrane

surface. Biological performance was also observed to have improved with PAC addition, evidenced by COD removal rate increases. However, the research could not address the question of whether PAC would become saturated and thus ineffective after a period of time.

In 2007, another study (Hu and Stuckey, 2007) examined the effect of the addition of activated carbon to three 3 L submerged AnMBRs. Performance of the AnMBRs was measured using COD removal, flux, and TMP. One reactor was operated as control with no activated carbon addition, one with 1.7 g/L of PAC, and the third with 1.7 g/L of granular activated carbon (GAC). While COD removal was as high as 90% in all three AnMBRs, in comparison to the control AnMBR, the average COD removal in the AnMBR with PAC increased by 22.4%, while the AnMBR with GAC was not significantly better. The difference in performance was attributed to the fact that PAC has a significantly greater surface area per mass than GAC, resulting in the greater absorbance of fine colloidal particles and high molecular weight organics onto the carbon surface. Also, the AnMBR with PAC exhibited lower TMPs and higher fluxes than both the AnMBR with GAC and the control AnMBR.

2.6 Future Research Needs

Literature review showed that very little research has been conducted on the operation of AnMBRs at psychrophilic temperatures. There is a lack of understanding on the effects of psychrophilic temperatures on the biological and physical performance of AnMBRs. In particular, membrane fouling control and mitigation mechanisms need to be explored further in order to improve the performance of AnMBRs at low temperatures. The benefits and selection of biofilm carriers inside the AnMBR should also be investigated further as biofilm carriers could be a potentially highly effective measure to reduce fouling. Overall, future research efforts need to focus on the investigation of the fouling behavior of membranes in AnMBRs under psychrophilic conditions as well as mitigation strategies in order to enable full-scale implementation in cold regions.

Chapter 3: Materials and Methods

3.1 AnMBR Configuration

In this study, three lab scale AnMBRs were used. Two AnMBRs were operated at psychrophilic temperatures while one was operated at room temperature. All three bioreactors had identical configuration. **Figure 1** presents a schematic diagram of each AnMBR.

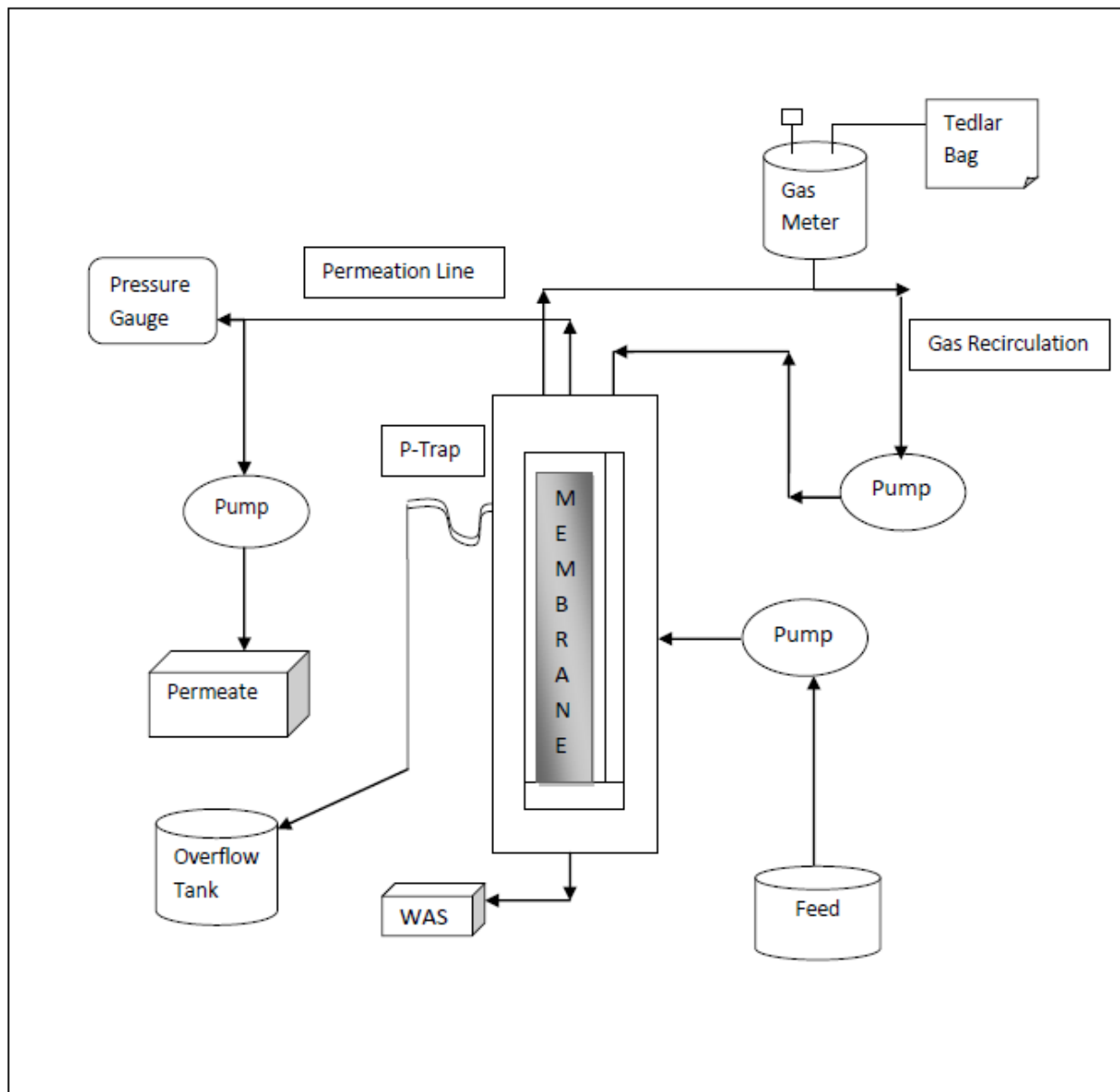


Figure 1: Schematic Diagram of the Lab Scale AnMBRs used in the study

Three 5 L reactor columns that incorporated submerged ZeeWeed® hollow fibre PVDF membranes with a nominal pore size of 0.04 µm and a nominal membrane surface area of 0.047 m² were employed. Temperature control was achieved by wrapping tubing along the reactor columns. The water inside the tubing was circulated through water baths that had cooling capacity. The overflow outlet was connected to a P-Trap that was partially filled with water to stop any biogas from exiting the bioreactor. In case of an overflow emergency, the P-Trap directed the surplus liquid to an overflow tank. Feed wastewater was supplied to the AnMBR through an opening near the middle of the bioreactor. A Stenner® peristaltic pump with a built in controller transferred the feed from a continuously mixed storage tank to the bioreactor. Waste biomass was wasted through an opening at the bottom of the bioreactor.

Permeate exited the top of the bioreactor through a line that had a pressure transducer that was connected to a Track-It® Data Logger integrated to measure transmembrane pressure (TMP). Gas sparging was employed to create surface shear to control membrane fouling. A Cole-Parmer® peristaltic pump extracted gas from the headspace above the mixed liquor and circulated it back to the system through the sparging stone that was attached to the bottom of the membrane module. To measure biogas production, a tipping bucket style gas flow meter manufactured at the University of Waterloo was added to the gas recirculation line through a T connection. A gas sampling port was installed into the gas recirculation line to facilitate sampling for gas composition. A 2 L Tedlar® gas sampling bag was connected to the gas meter to buffer pressure changes in the reactor during feeding, permeating, and sludge wasting. **Figure 2** presents the actual set up of two psychrophilic AnMBRs used in the study.

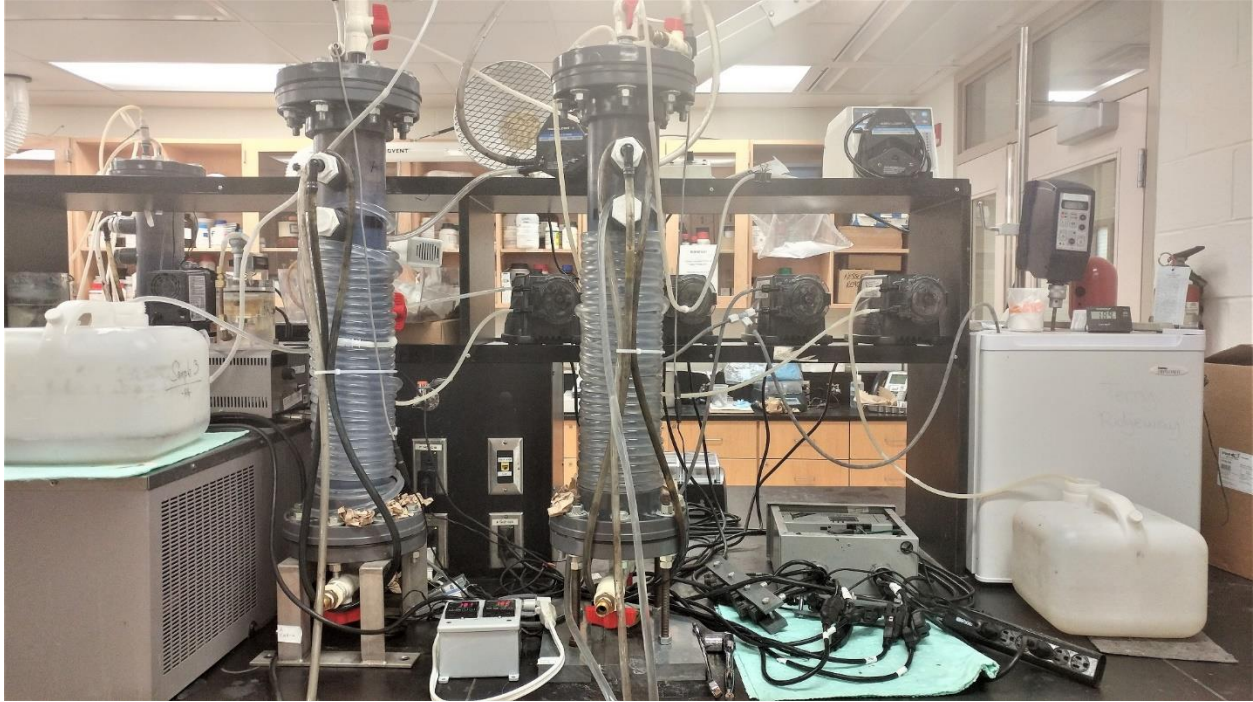


Figure 2: Actual set up of the psychrophilic AnMBRs

3.2 Operational Conditions

With the exception of temperature all three AnMBRs were operated under similar conditions throughout the study. Temperature was monitored using an OMEGA® PR-20 RTD temperature probe, which was inserted into each bioreactor through an opening on the wall. The output from the temperature probe was employed to inform a Dyna-Sense digital temperature controller that controlled the cooling water to the water jackets.

All AnMBRs had a solids residence time (SRT) of 30 days and a hydraulic residence time (HRT) of 0.4 days. The daily feed into the AnMBRs was pumped out of a wet well receiving municipal sewage from the City of Waterloo sanitary sewer line. Throughout the study, a volume of 10.13 L of wastewater was fed to each AnMBR, 0.130 L of Waste Sludge was manually wasted, and

10 L of permeate was generated daily. The AnMBRs were operated at a constant flux while TMP was monitored. The membranes were operated in a relaxed mode with 8 minutes of permeation followed by 2 minutes of relaxation. At a permeate flow rate of 10 L/d and a membrane surface area of 0.047 m², the flux was calculated from Equation 1 (Metcalf and Eddy, 2003) to be 8.87 LMH. The maximum flux recommended by Generic Electric was 12 LMH, which was above the flux adopted in this study.

$$\text{Flux} = \frac{\text{Permeate Flow Rate}}{\text{Membrane Surface Area}}$$

(Equation 1)

The mechanisms used to control membrane fouling included gas sparging, citric acid backwashing, and recovery cleaning of the membranes. Recovery cleaning of the membranes was conducted at the start of the study as well as between the two different phases. Recovery cleaning consisted of sequentially soaking each membrane in citric acid at 2 g/L and NaOCl at 2g/L for 16 hours respectively. Backwashing consisted of reversing the peristaltic pump and pumping permeate back through the pores of the membrane to the bioreactors. In situations where backwashing permeate was ineffective in reversing fouling, citric acid was used instead of the permeate to dislodge foulants.

3.3 Inoculum and Feed Characterization

Each bioreactor was inoculated with primary digester effluent obtained from the Galt Wastewater Treatment Plant (WWTP) located in Cambridge, Ontario. Because the primary

digester effluent had been anaerobically digested, it believed to contain a good culture of anaerobic bacteria. After large particles were screened out, 2 L of inoculum was introduced to each bioreactor along with 2 L of feed wastewater to achieve a total working volume of 4 L.

The municipal sewage flows continuously through a wet well and hence provided a well-mixed sewage. To ensure that the feed wastewater was fresh, the wet well was fully purged before feed was collected. Because the source of feed was continuously provided from the City’s main sanitary sewer line, it was assumed that the feed collected in this study would be representative of the City of Waterloo municipal wastewater characteristics. **Table 1** presents the characteristics of the feed wastewater that was employed in this study. The values presented in the table are representative of North American municipal wastewater as indicated in Metcalf and Eddy, 2003.

Table 1 Characteristics of Feed Wastewater

Parameters	Average Value	Standard Deviation
TCOD (mg/L)	373	54
SCOD (mg/L)	154	23
TSS (mg/L)	315	44
VSS (mg/L)	265	35
Sulfate (mg/L)	128	52
VFA-COD (mg/L)	12	3
pH	7.2	0.8

3.4 Experimental Design

The study started on January 5, 2015 when all three AnMBRs were configured to operational conditions and first inoculated. All three AnMBRs were receiving the same feed wastewater and running at room temperature initially. Over the period of the following 141 days, from January 5, 2015 to May 26, 2015, temperature control was introduced while steady state was slowly established. Steady state data collection began on May 27, 2015, which marks Day 1 of this research project. The experiment concluded on December 22, 2016, 576 days after the beginning of steady state data collection period. Throughout the 576 days, the study was conducted in three phases. During the initial phase of operation, the AnMBRs were operated at 24°C, 15°C and 10°C, while all other operational conditions were kept the same. The 24°C operation served as control while the 15°C and 10°C operations were designed to evaluate the impacts of lower temperature operation on AnMBR performance. During the second phase, the 15°C AnMBR from Phase 1 was lowered to 10°C to explore the reproducibility of the results from the AnMBR operating at 10°C. The 24°C operation remained the same. In the final phase of the study, Powdered Activated Carbon (PAC) was added to one of the AnMBRs operating at 10°C to achieve a concentration of 2 g/L. The PAC was added to the psychrophilic AnMBR as a biofilm carrier for potential biomass retention as well as a scouring agent to reduce membrane fouling. The 24°C AnMBR remained operation at the same temperature.

A summary of operational characteristics of the three AnMBRs from all three phases are summarized into **Table 2**.

Table 2 Summary of Operations

	Operating Temperature	Operational Variation	Parameters Monitored	Fouling Control Measures
Phase 1	AnMBR 1: 24°C AnMBR 2: 15°C AnMBR 3: 10°C	N/A	COD, VFA, CH ₄ , SO ₄ , TSS, VSS, pH, TMP	Gas sparging, Backwashing, Chemical Cleaning.
Phase 2	AnMBR 1: 24°C AnMBR 2: 10°C AnMBR 3: 10°C	AnMBR 2 is lowered to 10°C from 15°C. AnMBRs 1 and 3 remain unchanged.	COD, VFA, CH ₄ , SO ₄ , TSS, VSS, pH, TMP	Gas sparging, Backwashing, Chemical cleaning.
Phase 3	AnMBR 1: 24°C AnMBR 2: 10°C AnMBR 3: 10°C	PAC is added to AnMBR 3 at 2g/L. AnMBRs 1 and 2 remain unchanged.	COD, VFA, CH ₄ , SO ₄ , TSS, VSS, pH, TMP	Gas sparging, Backwashing, Chemical cleaning.

The operation of the AnMBRs began in May of 2015 and ended in December of 2016. **Table 3** provides a timeline of operations throughout the three phases of the study with the operation times relative to the starting date.

Table 3 AnMBR Operation Timeline

Operations	Start Date	End Date
Phase 1	Day 1	Day 310
Phase 2	Day 310	Day 468
Phase 3	Day 468	Day 576

3.5 Sampling Protocol

The feed (F), permeate (P), and waste activated sludge (WAS) streams from each AnMBR were sampled and analyzed three times a week to determine Total COD, Soluble COD, TSS, VSS, and VFA. The pH of WAS was measured daily to ensure the biological stability and robustness of each AnMBR. The pH measurement of WAS was taken at a higher frequency than the other parameters due to the fact that it was an indicator of methanogen activity in the bioreactor would. A significant drop in pH could be a warning sign that the mixed liquor inside the bioreactor had been too acidic for the methanogens to survive. In such a situation, sodium bicarbonate was added to neutralize the mixed liquor. **Table 4** shows the sampling schedule implemented during the study.

Table 4 Sampling Schedule

Parameter	Mon	Tues	Wed	Thurs	Fri	Sat/Sun
Total COD	F, P, WAS		F, P, WAS		F, P, WAS	
Soluble COD	F, P, WAS		F, P, WAS		F, P, WAS	
Sulfate, Nitrate	F, P		F, P		F, P	
TSS, VSS	F, P, WAS		F, P, WAS		F, P, WAS	
pH	F, P, WAS	WAS	F, P, WAS	WAS	F, P, WAS	WAS
VFA		F, P		F, P		

3.6 Sample Analysis

All analyses in this study were conducted according to Standard Method 5220 D (APHA, 1998). Each sample was measured in duplicates to characterize the reproducibility of the sampling and analyses processes.

3.6.1 Total COD

Prior to preparing sample vials for COD analysis, a calibration curve was established using stock standards. Five standards were made from COD stock standard (1000 mg/l) by dilution. Once standards were prepared and digested, a calibration curve was established to calibrate a HACH DR/2010 spectrophotometer. To determine the TCOD of a sample, 50 mL of the sample was first homogenized for 30 seconds. A volume of 2.5 mL of the homogenized sample was then added to a COD vial containing 1.5 mL of COD digestion solution and 3.5 mL of sulfuric acid reagent. In cases where the sample was too concentrated to be analyzed by the spectrophotometer, an appropriate dilution was applied, which was accounted for after measurements were taken. After sample was added to the vial, the vial was mixed by inverting it several times and then placed in the preheated HACH COD block digester for 3 hours at 150°C. Once the samples were cooled to room temperature, they were measured at 600 nm using a HACH DR/2000 Spectrophotometer. For each batch of COD analysis, a blank was prepared by transferring 2.5 ml of deionized water to a COD vial containing COD acid reagent and COD digestion solution.

3.6.2 Soluble COD

To determine the Soluble COD of a sample, 50 mL of the sample was centrifuged for 30 minutes. The supernatant was then filtered through a Whatman Glass Microfibre filter (934-AH) with a pore size of 1.5 μm . Once 5 ml of filtrate was collected, it was prepared for digestion and analysis according to the same procedure described in Section 3.6.1 Total COD.

3.6.3 Suspended Solids

Total and volatile suspended solids were analyzed in this study according to Standard Methods 2540 D and E, respectively (APHA, 1998). To measure the suspended solids of a sample, an aluminum weighing dish with a 1.5 μm Whatman Glass Microfibre filter (934-AH) placed in it was dried at 550°C for 45 minutes. Once it cooled, the combined weight of the dish and the filter paper was recorded. Then 5 mL of the sample was filtered and 10 mL of deionized water was added to ensure all solid particles were captured on the filter. The filter was then dried at 105°C for a day and weighed along with the dish. The increase in mass from the initial weight was employed to calculate the TSS. The same filter was then combusted at 550°C for an hour. After the sample cooled, the weight was recorded to calculate non-volatile suspended solids. The difference between total and non-volatile suspended solids was the amount of mass lost to combustion at 550°C, which was the desired VSS value.

3.6.4 Volatile Fatty Acids

The determination of volatile fatty acids (VFAs), including acetic, propionic, butyric, isobutyric, valeric, and isovaleric acids, was done by gas chromatography (GC) (Model: Hewlett Packard HP 5890 Series II) equipped with a Nukol fused-silica capillary column and flame ionization

detector (FID). Helium gas was used as a carrier gas. Samples were filtered using MF-Millipore™ Membrane Filters with a 0.45 µm pore size. Each sample was acidified to pH 2 using 1 N phosphoric acid before GC-FID analyses. A 1.5 ml glass vial with septa cap (Sigma-Aldrich) was used to contain each sample. The vial was shaken for 30 seconds using a shaker to ensure adequate mixing. A series of VFA standards for the calibration curves were prepared using dilution of a stock solution. The initial temperature of the column was 110 °C, increasing to 195 °C at the rate of 8 °C/min, and then held constant at the final temperature of 195 °C for 9 min. Injector and detector temperatures were 220 °C and 280 °C, respectively.

3.6.5 Sulfate

Sulfate concentrations in feed and permeate streams were measured using Suppressed Ion Chromatography following ASTM Standard Test Method for Anions in Water (ASTM, 2016). Samples were prepared using filtrate from the SCOD analysis. Each sample was pumped through two columns, a suppressor device, and into a conductivity detector. The analytical column was a Dionex IonPac AS4A-SC Analytical (4 x 250 mm) and the guard column was a Dionex IonPac AG4A-SC Guard (4 x 50 mm). Quantitation was accomplished by measuring the area under each peak and comparing it to a calibration curve generated from known standards. Ambient temperature was adopted while conducting the analysis. The applied current was 32 mA and the injection volume was 25 µL per sample. All samples were measured in duplicates.

3.6.6 pH

The pH of each sample was measured daily using an Omega PHB-600R pH Benchtop Meter. To prevent cross contamination, the pH probe was rinsed thoroughly between samples.

Chapter 4: Results and Discussion

In this chapter, results obtained from the study are presented, in terms of both biological and physical performance evaluations of the AnMBRs. Biological performance is evaluated using COD removal efficiency, VFA accumulation, and Methane production in each AnMBR. The metric for physical performance is whether TMP increases were observed during operation.

Section 4.1 presents biological performance results from the entire study including Phases 1 to 3. Section 4.2 presents detailed results from Phase 1 including COD removal, VFA accumulation, and methane production. Sections 4.3 and 4.4 present detailed results from Phase 2 and Phase 3 respectively. Data presented in this chapter have been synthesized and statistically analyzed to obtain a quantitative understanding of the overall effect of lowering operating temperatures in AnMBRs. All raw data collected throughout the study are available in Appendix A to Appendix C.

4.1 Overall Biological Performance

Throughout the study, data were collected on TCOD, SCOD, TSS, VSS, VFA, biogas production, pH and TMP. To compare the three operations over three phases of the study, the influent COD concentration and the effluent COD concentration of each AnMBR were plotted and presented in **Figure 3**.

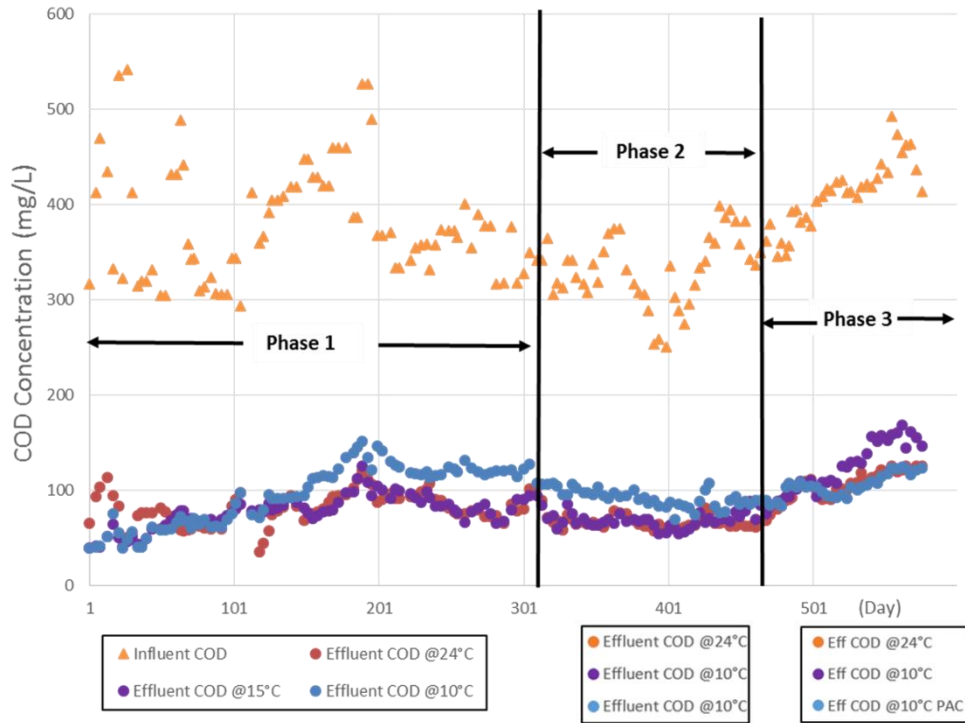


Figure 3 Influent vs Effluent COD Concentrations throughout the Study

It can be observed that during phase 1, the effluent COD of the 10°C AnMBR showed a much higher concentration than the effluent COD of the control AnMBR, which was the 24°C AnMBR. The 15°C AnMBR produced effluent of similar quality to the control AnMBR. In Phase 2, the 10°C AnMBR from Phase 1 continued to show higher effluent COD than the control AnMBR. However, even though the temperature of the 15°C AnMBR from Phase 1 was lowered to 10°C in Phase 2, its effluent quality remained similar to that of the control AnMBR for some time. This may have been due to a continued high level of activity of the biomass from the 15°C operation for some time after the temperature shift. In phase 3, all effluent COD concentrations increased in response to the increased influent COD.

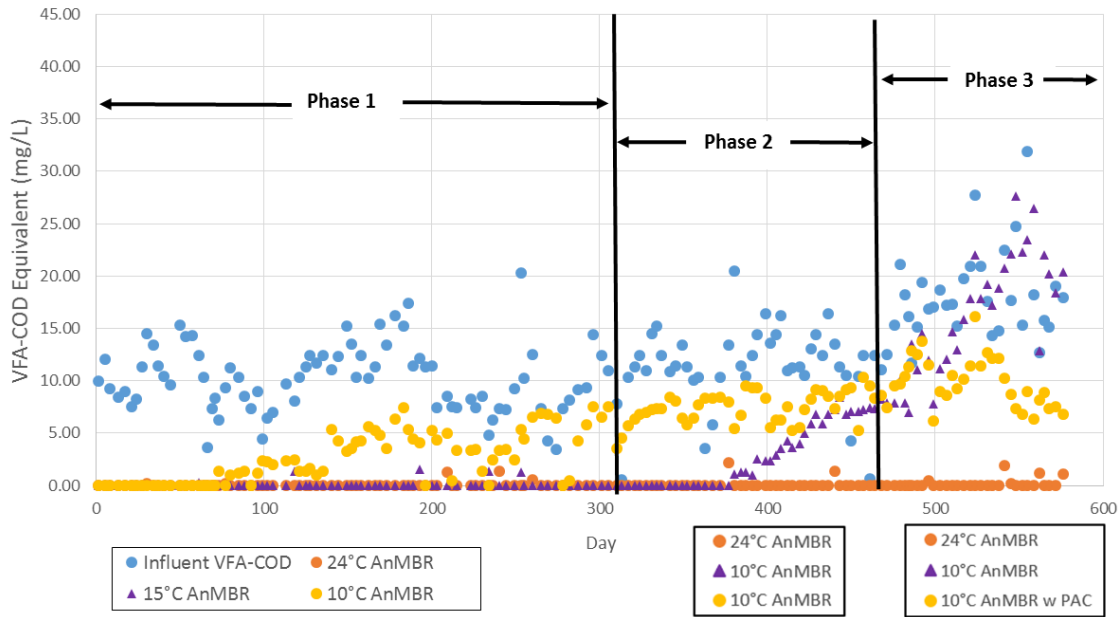


Figure 4 Influent vs Accumulated VFA throughout the Study

Figure 4 shows the VFA accumulation inside the three bioreactors throughout the three phases.

Anaerobic degradation of complex pollutants in wastewater involves four stages: hydrolysis, acidogenesis, acetogenesis, and methanogenesis. Volatile fatty acids (VFA) are intermediates formed by acidogenic bacteria during acidogenesis, which can be subsequently converted to acetate, CO₂ and H₂ by acetogenic bacteria. An accumulation of VFAs in an anaerobic environment can indicate a lowered utilization rate by methanogenic bacteria. If the VFA production rate exceeds the VFA utilization rate, the pH of the system can decrease and result in further reduced activity of the methanogens; thereby decreasing their use of acetic acid and hydrogen gas, causing a further accumulation of VFAs (Metcalf and Eddy, 2003).

In the current study bicarbonate was used as a buffering agent to control and regulate the pH levels throughout the study. VFA data were therefore collected to compare the biological performance of each AnMBR and are presented in **Figure 4**. No VFA accumulation was

observed in the 24°C AnMBR throughout the entire study. In Phase 1, the 15°C AnMBR also showed no VFA accumulation. However, once the temperature had been lowered from 15°C to 10°C, VFA accumulation was observed and it continued to climb. Accumulation of VFAs can occur during times of stress such as higher loading rates and drastic operating environment changes. In this study however, the loading rate was maintained constant, suggesting that there is a correlation between unconsumed VFA and operating temperatures. In an anaerobic environment, complex organics are broken down into a mixture of VFAs, mostly acetic, propionic, and butyric acids, by acidogens. Acidogens are a consortium of hydrolytic and acidogenic bacteria. VFAs are then converted to carbon dioxide and methane by acetogenic bacteria and methanogenic archaea (Doble & Kumar, 2005). Any VFA accumulation inside the bioreactor is an indication that the conversion to carbon dioxide and methane may not be successful or that there is an imbalance between VFA production and VFA utilization. As temperature is lowered, microbial activities are slowed down, especially methanogens, resulting in the imbalance.

It was also observed that following VFA accumulation, the pH inside the bioreactor was decreased. In an effort to maintain pH as an operational parameter, sodium bicarbonate was added to the bioreactor to bring the pH back to neutral.

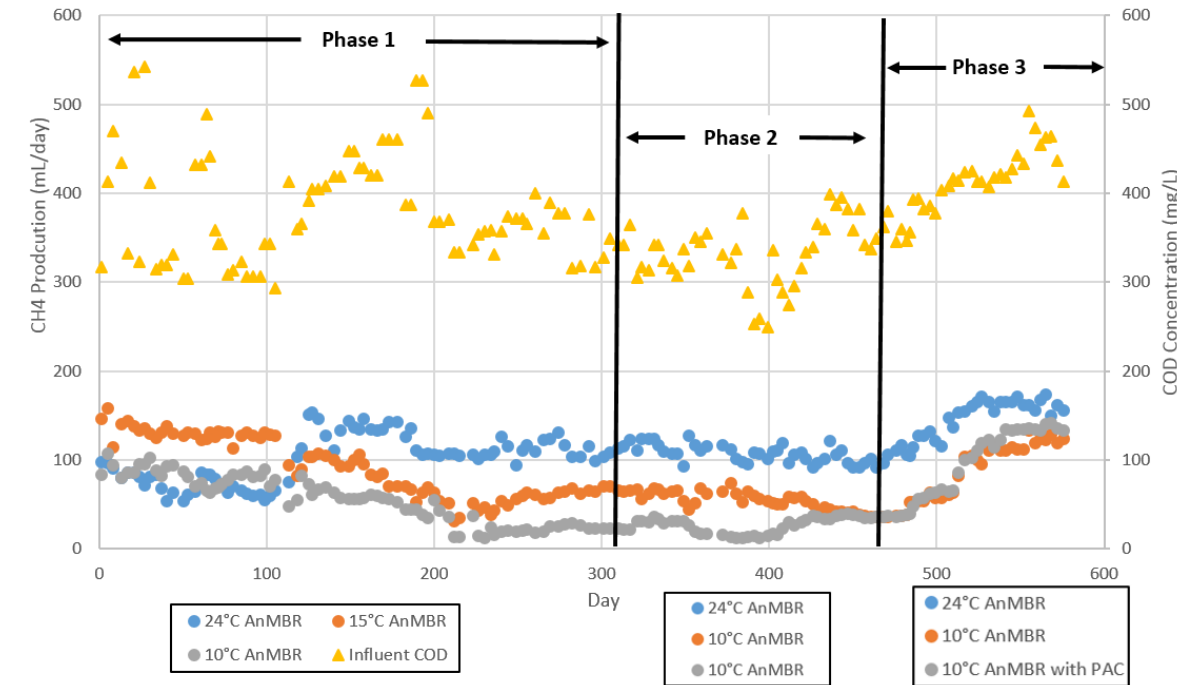


Figure 5 Influent COD vs CH₄ Production throughout the Study

Figure 5 presents the methane production results from all three phases of the study. Throughout the study, all three AnMBRs had lower methane production than theoretical methane production values calculated assuming 350 L of methane was generated per kg of COD removed (Grady et al. 2011). This could be due to the presence of high concentrations of sulfate in the feed as shown in **Table 5**.

Table 5 Steady State Influent Sulfate Concentrations throughout the Study

	Steady State Period	Influent Sulfate Concentration (mg/L)
Phase 1	Day 151 - 310	117.95 ± 57.35
Phase 2	Day 380 - 468	128.14 ± 82.39
Phase 3	Day 520 - 576	90.71 ± 12.86

The high levels of sulfate in the influent greatly impacted biogas production as methanogens and sulfate reducers compete for substrates. Also, dissolved methane was observed in the permeate from each AnMBR, indicating that a fraction of the methane generated by the anaerobic process was lost through permeate instead of being collected in the headspace. The findings agree with observations reported in literature. For example, when Smith et al. (2014) operated psychrophilic AnMBRs, the reported biogas production was limited by sulfate reduction, the wastewater's low strength, the high methane solubility at the low operational temperature, and methane oversaturation in the permeate. Smith et al. (2014) reported that approximately 40-50% of the total methane generated in the AnMBR was dissolved in the permeate and was thus discharged with the permeate rather than collected in the headspace. However, it was consistently shown that the 24°C AnMBR had higher methane production than both the psychrophilic AnMBRs, even after PAC addition.

4.2 Phase 1 AnMBR Performance

During Phase 1 of the study, steady state was determined to have been established around Day 151. **Table 6** summarizes the average steady state COD removals at the three different temperatures. The 24°C AnMBR had the highest removal rate, at 78.3% corresponding to an average permeate COD of 83.0 mg/L. The 15°C AnMBR had the second highest average COD removal, at 77.3% and the 10°C AnMBR had the lowest COD removal, at 69.8% corresponding to a permeate COD of 115.2 mg/L.

Table 6 Phase I Summary of COD removals and permeate COD concentrations

	Average COD Removal	% Change from Control	Permeate COD (mg/L)
24°C	78.3 ± 4.5 %	N/A	83.0 ± 13.4
15°C	77.3 ± 3.9 %	1.3% Decrease	86.8 ± 11.8
10°C	69.8 ± 5.8 %,	10.9% Decrease	115.2 ± 17.4

To statistically compare the removal efficiencies of the three AnMBRs, a one-way analysis of variance (ANOVA) was completed on the average COD removal efficiencies. Results from the analysis are shown below in **Figure 6**. The null hypothesis was that all three average removal efficiencies were equal. It can be seen from the ANOVA summary that the F value (46.51) was greater than F crit (3.06), therefore the null hypothesis was rejected. It was concluded that the average COD removal efficiencies of the three AnMBRs were not all equal and at least one of the average removal efficiencies was different.

SUMMARY						
Groups	Count	Sum	Average	Variance		
Column 1	51	3991.33	78.26	20.80		
Column 2	51	3942.33	77.30	15.38		
Column 3	51	3560.56	69.81	34.18		
ANOVA						
Source of Variation	SS	df	MS	F	P-value	F crit
Between Groups	2181.18	2.00	1090.59	46.51	0.00	3.06
Within Groups	3517.51	150.00	23.45			
Total	5698.69	152.00				

Figure 6 ANOVA Summary on Phase 1 Average COD Removal Efficiencies

To further compare the average removal efficiencies of all three operations, a Tukey’s test was applied simultaneously to all three pairwise comparisons: 24°C vs 15°C, 24°C vs 10°C, and 15°C vs 10°C. Results from the Tukey’s test are shown below in **Figure 7**.

q(24°C,10°C)	=	12.46					
df	=	150					
qCritical (from Studentized Range)	=	3.31					
q(24°C,10°C) > qCritical	The difference between the two means is significant at a significance level of 0.05.						
q(24°C,15°C)	=	1.42					
df	=	150					
qCritical (from Studentized Range)	=	3.31					
q(24°C,15°C) < qCritical	The difference between the two means is NOT significant at a significance level of 0.05.						
q(15°C,10°C)	=	11.04					
df	=	150					
qCritical (from Studentized Range)	=	3.31					
q(15°C,10°C) > qCritical	The difference between the two means is significant at a significance level of 0.05.						

Figure 7 Tukey Test Summary on Phase 1 Average COD Removal Efficiencies

The Tukey’s test shows that at a significance level of 0.05, the average COD removal efficiencies between the 24°C and 10°C AnMBRs were significantly different; the average COD removal efficiencies between the 15°C and 10°C AnMBRs were significantly different; however, the average COD removal efficiencies between the 24°C and 15°C AnMBRs were not significantly different. Therefore it was concluded that temperature did not affect removal efficiency over the range of 24°C to 15°C; however, removal efficiency declined significantly from 15°C to 10°C.

A steady state COD cumulative analysis was conducted for each AnMBR during each phase. A COD mass balance was conducted using the following equation:

$$\text{COD}_{\text{feed}} = \text{COD}_{\text{mass out}} + \text{accumulation}$$

$$\text{where, } \text{COD}_{\text{mass out}} = \text{COD}_{\text{WAS}} + \text{COD}_{\text{SO}_4} + \text{COD}_{\text{perm}} + \text{COD}_{\text{CH}_4}$$

The accumulation of high-molecular-weight organic compounds is a common phenomenon in membrane bioreactors. It is a result of biological processes inside the bioreactor and it causes the COD accumulation to increase over an extended period of operation (Schalk and Kuhn, 2014). The sum of all COD-bearing streams exiting the AnMBR plus the accumulation in the AnMBR for the 24°C operation was plotted in **Figure 8** along with the mass of COD entering the MBR to assess the quality of the data by examining the mass balance closure. The COD streams exiting the MBR included sulfate reduction, permeate, waste activated sludge (WAS), and methane (CH₄). Cumulative plots were generated for the 15°C and 10°C AnMBR following the same approach. In **Figure 8**, COD mass is represented on the y-axis. Therefore, the following interpretation applies to the figure:

$$\text{COD}_{\text{feed}} = y(\text{feed})$$

$$\text{COD}_{\text{mass out} + \text{accumulation}} = y(\text{mass out} + \text{accumulation}) \text{COD}_{\text{WAS}} = y(\text{WAS})$$

$$\text{COD}_{\text{SO}_4} = y(\text{SO}_4)$$

$$\text{COD}_{\text{perm}} = y(\text{perm})$$

$$\text{COD}_{\text{CH}_4} = y(\text{CH}_4)$$

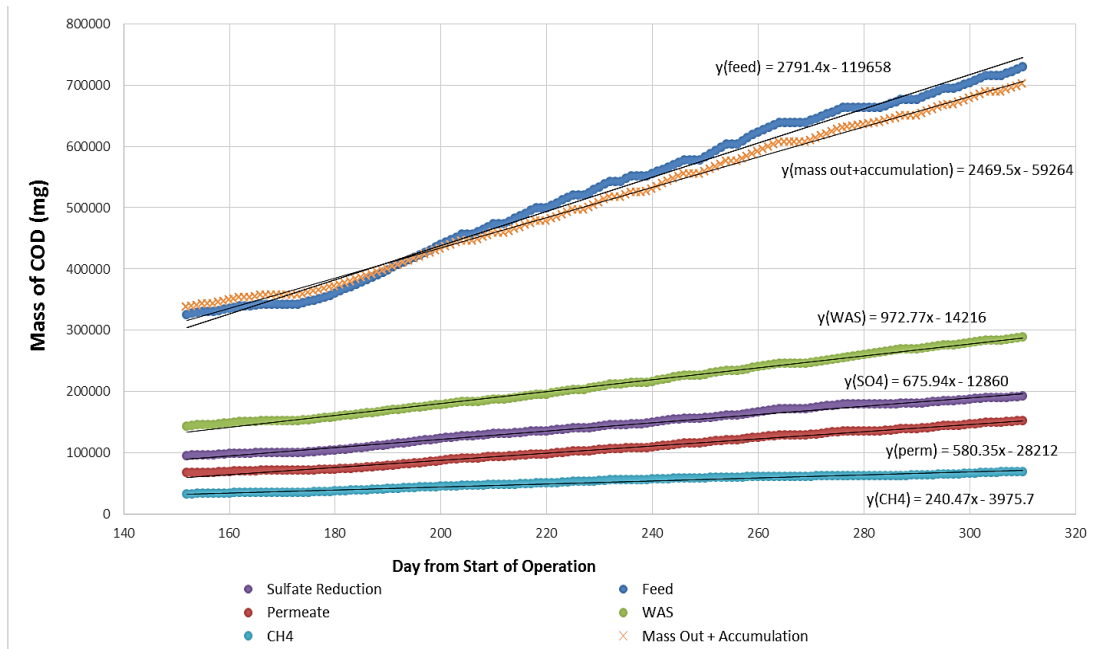


Figure 8 Phase 1 COD Mass Balance for the 24°C MBR

The cumulative mass of feed COD was calculated by adding the daily mass of COD to the accumulated mass of COD from the start of MBR operation. Similarly, the cumulative masses of permeate COD and WAS COD were found through the cumulative addition of COD in each respective stream from the start of the AnMBR operation. To obtain the cumulative mass of COD consumed in sulfate reduction, sulfate concentrations in the feed and permeate streams were measured to determine the concentration of sulfate reduced. The concentration of reduced sulfate was then converted to COD mass equivalent to obtain the cumulative COD consumed in sulfate reduction using the same approach for the feed, permeate, and WAS streams discussed in this section. Observed daily methane (CH₄) production was converted to COD mass equivalent, and then used to find the cumulative mass from the start of AnMBR operation. It can be seen in **Figure 8** that the line representing COD_{mass out + accumulation} positions very closely to the line representing COD_{feed}. In a theoretical COD mass balance, the two lines would be overlapping

each other with no deviation. In this study, deviation could be attributed to a less than perfect COD mass balance closure caused by several factors including experimental errors and the unmeasured methane saturated in permeate as a lost stream of COD. In future studies, it is recommended to develop a method to measure saturated methane in permeate.

The slope of each COD bearing stream was determined and used to determine the fractions of total influent COD that were present in each effluent destination. The fractions are presented in

Table 7.

Table 7 COD Fractions of All COD Bearing Streams during Phase 1

	24°C	15°C	10°C
f_{WAS}	34.9%	33.5%	38.9%
f_{PERM}	20.8%	22.9%	32.4%
f_{CH_4}	8.6%	4.6%	2.2%
f_{SO_4}	24.2%,	29.4%	28.0%
$f_{\text{mass out+accum}}$	88.5%	88.6%	100.5%

From **Table 7** it can be seen that the the sum of the fractions of all COD mass out plus the accumulation term indicate good COD mass balance closure, providing confidence in the analysis of COD fate through the reactor. The relatively small lack of mass balance closure may have been due to oversaturation of methane in the permeate. It can be observed that as temperature decreased from 24°C to 10°C, the fraction of COD converted to CH₄ decreased. Further, as the temperature decreased, the fraction of COD in the permeate (f_{perm}) increased confirming a reduction in COD consumed by microorganisms.

VFA data were collected to compare the biological performance of each AnMBR in Phase 1 and are presented in **Figure 9**. As seen in **Figure 9**, an increasing and decreasing pattern of the

effluent VFA-COD that closely resembled that of the influent VFA-COD was observed at steady state in the 10°C AnMBR. This pattern suggests that the methanogen population was unable to convert all the VFAs that were generated under higher influent COD loadings.. The pattern of permeate VFA concentrations was consistent with the pattern observed for permeate COD, indicating that the soluble COD in the permeate was due to the presence of VFA.

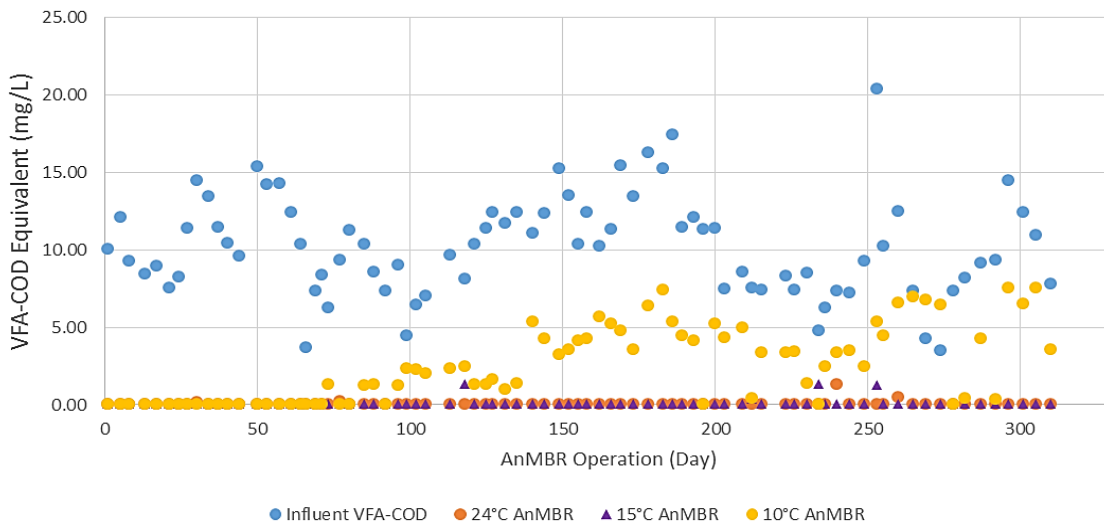


Figure 9 Phase 1 Influent vs Effluent VFA-COD

Steady state in Phase 1 was determined to have been established around Day 151. **Table 8** summarizes the average steady state VFA-COD concentrations at the three different temperatures.

Table 8 Phase 1 Steady State VFA-COD Concentrations

	Average VFA-COD Concentration (mg/L)	Percent Change from Control
24°C	0.04 ± 0.16	N/A
15°C	0.12 ± 0.28	2% Increase
10°C	3.96 ± 2.39	98% Increase

As seen in **Table 8**, the 10°C AnMBR had measurable concentrations of VFA in the permeate after steady state was established. The 24°C and 15°C AnMBRs both exhibited insignificant

amounts of VFA compared to the 10°C AnMBR. The high standard deviations in all three data sets could be attributed to the variation in influent COD. As previously discussed, the variation resembled the fluctuation in influent COD, suggesting that the methanogen population was unable to convert all the VFAs that were generated under higher influent COD loadings.

Methane production data were collected during Phase 1 and presented in **Figure 10**. It can be seen that after steady state was determined to have been established around Day 151, the three bioreactors produced differing quantities of methane. The 24°C AnMBR had the highest methane production, followed by the 15°C AnMBR. The 10°C AnMBR had the lowest methane production. Influent COD is also presented in the figure to compare with the patterns in methane production. It can be seen that a period of high influent COD was followed by a rise in methane production in all three AnMBRs.

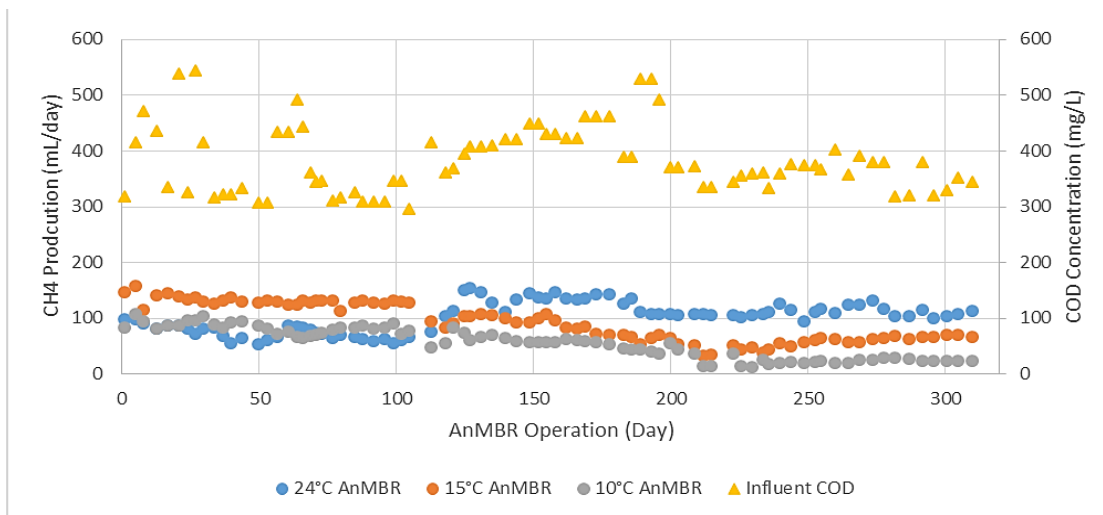


Figure 10 Phase 1 Methane Production Results

Table 9 summarizes the average steady state methane productions in mL/d at the three different temperatures. As seen in **Table 9**, the 24°C AnMBR had the highest average methane

production, followed by the 15°C AnMBR. The 10°C AnMBR had the lowest average methane production. The high standard deviations in all three data sets could be attributed to the variation in influent COD. All three AnMBRs had lower methane production than theoretical methane production values calculated assuming 350 L of methane was generated per kg of COD removed (Grady et al. 2011). This was likely due to the presence of high concentrations of sulfate (117.95 ± 57.35 mg/L) in the feed.

Table 9 Phase 1 Steady State Methane Productions

	Average Methane Production (mL/d)	Percent Change from Control
24°C	117 ± 27	N/A
15°C	71 ± 34	39.3% Decrease
10°C	40 ± 27	65.8% Decrease

4.3 Phase 2 AnMBR Performance

During the second phase of the study, one AnMBR was maintained at 24°C while two AnMBRs were operated at 10°C. Both of the two psychrophilic AnMBRs at 10°C exhibited decreased permeate quality, lowered biogas production, and unconsumed volatile fatty acids. Phase 2 steady state was determined to have been established around Day 380. **Table 10** summarizes the average COD removals from the three AnMBRs after steady state was established.

Table 10 Phase 2 Summary of COD removals and permeate COD concentrations

	Average COD Removal	% Change from Control	Permeate COD (mg/L)
24°C	80.2 ± 2.5 %	N/A	64.4 ± 5.0
10°C ¹	79.3 ± 2.2 %	1.1% Decrease	67.8 ± 8.5
10°C	73.4 ± 3.9 %	8.5% Decrease	86.4 ± 7.5

Notes:

1. Previously operated at 15°C during Phase 1 of the study.

To statistically compare the removal efficiencies of the three AnMBRs, a one-way analysis of variance (ANOVA) was completed on the average COD values. Results from the analysis are shown below in **Figure 11**. The null hypothesis was that all three average removal efficiencies were equal. It can be seen from the ANOVA summary that $F (39.07) > F \text{ crit } (3.12)$, therefore the null hypothesis was rejected. It was concluded that the average COD removal efficiencies of the three AnMBRs were not all equal and at least one of the average removal efficiencies is different.

SUMMARY						
<i>Groups</i>	<i>Count</i>	<i>Sum</i>	<i>Average</i>	<i>Variance</i>		
Column 1	26	2084.55	80.17	6.28		
Column 2	26	2061.42	79.29	5.09		
Column 3	26	1907.35	73.36	16.03		
ANOVA						
<i>Source of Variation</i>	<i>SS</i>	<i>df</i>	<i>MS</i>	<i>F</i>	<i>P-value</i>	<i>F crit</i>
Between Groups	713.7072666	2	356.85	39.07	0.00	3.12
Within Groups	685.0697447	75	9.13			
Total	1398.777011	77				

Figure 11 ANOVA Summary on Phase 2 Average COD Removal Efficiencies

To further compare the average removal efficiencies of all three operations, a Tukey’s test was applied simultaneously to all three pairwise comparisons: 24°C vs 10°C, 24°C vs 15°C (previously 15°C), and 10°C (previously 15°C) vs 10°C. Results from the Tukey’s test are shown below in **Figure 12**.

q(24°C,10°C)	=	11.50				
df	=	75				
qCritical (from Studentized Range)	=	3.38				
q(24°C,10°C) > qCritical	The difference between the two means is significant at a significance level of 0.05.					
q(24°C,10°C*)	=	1.50				
df	=	75				
qCritical (from Studentized Range)	=	3.38				
q(24°C,10°C*) < qCritical	The difference between the two means is NOT significant at a significance level of 0.05.					
q(10°C*,10°C)	=	10.00				
df	=	75				
qCritical (from Studentized Range)	=	3.38				
q(10°C*,10°C) > qCritical	The difference between the two means is significant at a significance level of 0.05.					
*Previously operated at 15°C in Phase 1						

Figure 12 Tukey Test Summary on Phase 2 Average COD Removal Efficiencies

The Tukey's test shows that at a significance level of 0.05, the average COD removal efficiencies between the 24°C and 10°C AnMBRs were significantly different; it was therefore concluded that removal efficiency declined significantly from 24°C to 10°C. The Tukey results also show that the average COD removal efficiencies between the 24°C and 10°C (previously 15°C) AnMBRs were not significantly different. Therefore it was concluded that temperature did not affect removal efficiency when the 15°C AnMBR was lowered to 10°C. Even though the 15°C AnMBR from Phase 1 was lowered to 10°C in Phase 2, its effluent quality remained very similar to that of the control AnMBR. This AnMBR had similar removal capability to the control AnMBR possibly because the microbes established at 15°C AnMBR had not entirely lost their ability to breakdown organics after the temperature shift. The 10°C AnMBR had the lowest COD removal, which agreed with the literature that demonstrated that as the operating temperature of an AnMBR is reduced, AnMBR performance declines resulting in decreased permeate quality. Specifically, Chu et al. (2005) operated AnMBRs at 25°C, 20°C, 15°C, and 11°C and observed a decreasing COD removal from 93-96% to 76-81% as temperature dropped.

Ho and Sung (2010) also reported decreased COD removal from 95% to 85% when the operating temperature of AnMBRs changed from 25°C to 15°C.

COD mass balance was conducted using the following equation:

$COD_{\text{feed}} = COD_{\text{mass out + accumulation}}$, where

$COD_{\text{mass out}} = COD_{\text{WAS}} + COD_{\text{SO}_4} + COD_{\text{perm}} + COD_{\text{CH}_4}$

The cumulative mass of COD versus time in COD-bearing streams exiting the AnMBR plus the accumulation in the AnMBR for the 24°C operation was plotted in **Figure 13** along with the cumulative mass of COD entering the MBR to assess the quality of the data by examining the mass balance closure. The COD streams exiting the MBR included sulfate reduction, permeate, waste activated sludge (WAS), and methane (CH₄). The approach used for the Phase 1 COD cumulative mass balance described in Section 4.2 was applied to Phase 2 COD data. **Figure 13** shows the sum of all streams leaving the bioreactor plus the accumulation inside the bioreactor was only slightly less than the COD entering the bioreactor, showing a good COD balance.

In **Figure 13**, COD mass is represented on the y-axis. Therefore, the following interpretation applies to the figure:

$COD_{\text{feed}} = y(\text{feed})$, dark blue line

$COD_{\text{mass out + accumulation}} = y(\text{mass out + accumulation})$, orange line

$COD_{\text{WAS}} = y(\text{WAS})$, green line

$COD_{\text{SO}_4} = y(\text{SO}_4)$, purple line

$COD_{\text{perm}} = y(\text{perm})$, red line

$COD_{\text{CH}_4} = y(\text{CH}_4)$, light blue line

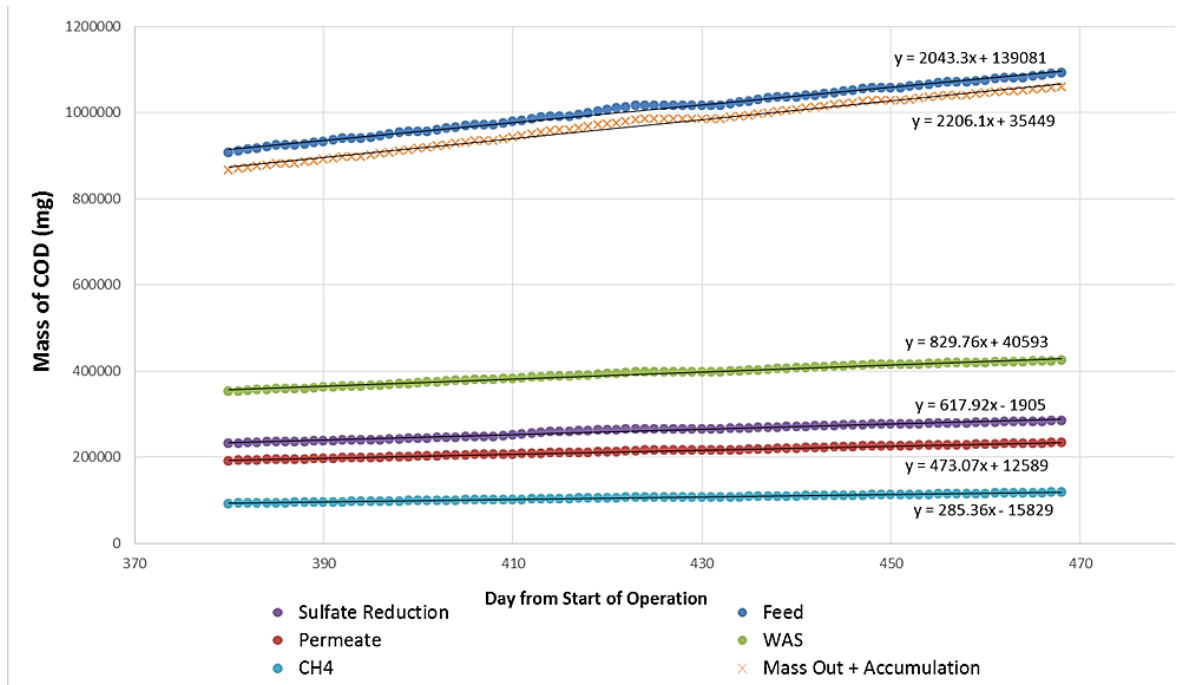


Figure 13 Phase 2 Steady State COD Mass Balance for the 24°C MBR

It can be seen in **Figure 13** that the line representing $COD_{\text{mass out + accumulation}}$ positions slightly below the line representing COD_{feed} . In a theoretical COD mass balance, the two lines would be overlapping each other with no deviation. In this study, deviation could be attributed to a less than perfect COD mass balance closure caused by several factors including experimental errors and the unmeasured methane saturated in permeate as a lost stream of COD. In future studies, it is recommended to develop a method to measure saturated methane in permeate.

Cumulative COD plots for the two 10°C AnMBRs were generated using the same approach. The slope of each COD bearing stream was determined and used to derive the destination fractions of COD entering the system as shown in **Table 11**. Mass balance closure was within +/- 10% for the 24°C and 10°C¹ operations. For the 10°C operation, mass balance closure was 84.4%. The

lack of mass balance closure in the 10°C AnMBR may have been due to increased oversaturation of methane in the permeate as temperature lowered.

Table 11 COD Fractions of All COD Bearing Streams during Phase 2

	24°C	10°C ¹	10°C
f_{WAS}	40.6%	32.7%	27.9%
f_{PERM}	23.2%	26.0%	30.2%
f_{CH_4}	14.0%	7.4%	3.8%
f_{SO_4}	30.2%	27.2%	24.7%
$f_{\text{mass out+accum}}$	108.0%	90.7%	84.4%

Notes:

1. Previously operated at 15°C during Phase 1 of the study.

It can be observed from **Table 11** that the 24°C AnMBR had the highest fraction of methane conversion from COD. As temperature decreased from 24°C to 10°C, the fraction of COD converted to CH₄ decreased. As temperature decreased, f_{PERM} increased indicating that more soluble COD ended up in the permeate instead of being consumed by microorganisms. Also, biomass retention inside the bioreactor decreased as the temperature decreased, as reflected in f_{WAS} . Overall, the COD fractionation analysis shows that a decrease in operating temperature resulted in less COD being converted to CH₄, more COD ending up in the permeate stream, and lowered biomass retention inside the bioreactor. It is worth noting that the fraction of COD converted to SO₄ is greater than the COD converted to CH₄. The presence of high concentrations of sulfate in the feed resulted in the large fraction of COD consumed by sulfate, which reduced the amount COD available for methanogens to convert COD to methane.

VFA data were collected to compare the biological performance of each AnMBR in Phase 2 and are presented in **Figure 14**. **Figure 14** shows that the 10°C AnMBR that was previously operated at 15 °C started to accumulate VFA after steady state was established. From Day 380 when

steady state was established, VFA accumulation continued to climb and reached a max concentration of 8.4 mg/L on Day 443. The 10°C AnMBR consistently had a high VFA accumulation, exceeding that of the control and previously 15°C AnMBRs, and reaching a max concentration of 10.4 mg/L on Day 457. Similar to Phase 1, small amounts of VFA were detected in the 24°C AnMBR but this was not significant enough to suggest VFA accumulation due to an imbalance between VFA production and utilization.

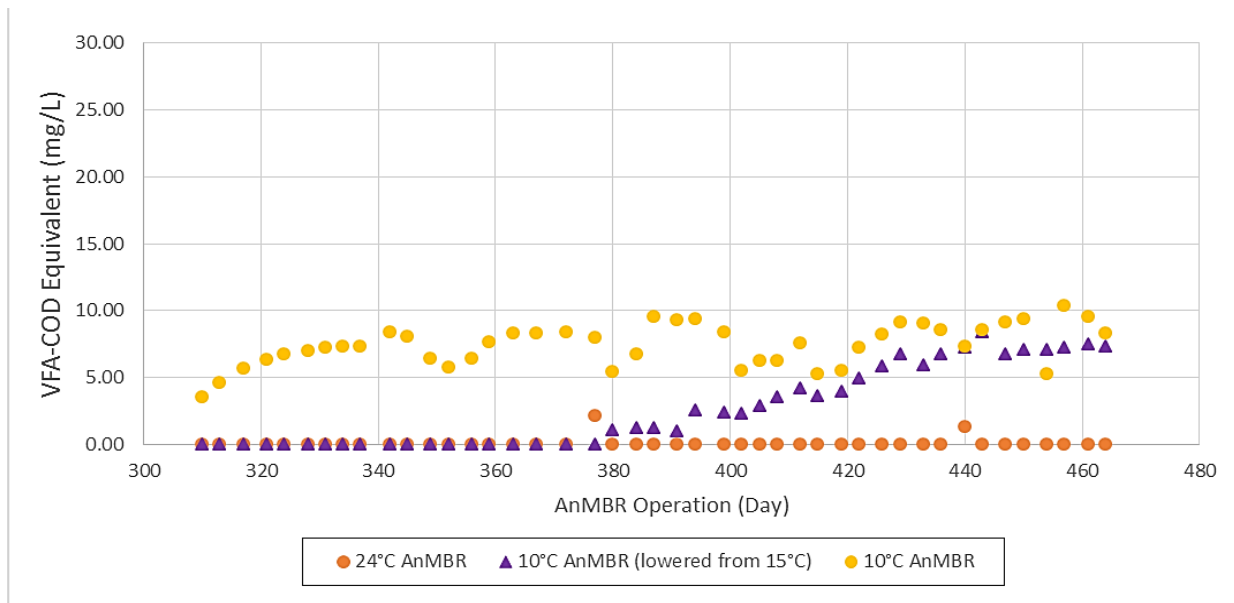


Figure 14 Phase 2 Influent vs Effluent VFA-COD

Table 12 summarizes the average steady state VFA-COD concentrations at the three different temperatures. The average VFA-COD concentrations at steady state show that the 10°C AnMBR had the highest accumulation of acids and the previously 15°C AnMBR also started to accumulate acids as operation temperature dropped to 10°C. This data confirmed the lower utilization rate by methanogenic bacteria in the 10°C AnMBRs.

Table 12 Phase 2 Steady State VFA-COD Concentrations

	Average VFA-COD Concentration (mg/L)	Percent Change from Control
24°C	0.05 ± 0.26	N/A
10°C ¹	4.74 ± 2.33	93.8% Increase
10°C	7.84 ± 1.56	155.8% Increase

Notes:

1. Previously operated at 15°C during Phase 1 of the study.

Methane production data were collected during Phase 2 and presented in **Figure 15**. Steady state was determined to have been established around Day 380. It can be observed that when temperature was lowered from 15°C to 10°C for the 10°C AnMBR, methane production started to decrease. There was not much change in the methane production from the 24°C AnMBR. The previously 10°C AnMBR continued to show low methane production throughout Phase 2. Influent COD is also presented in the figure to compare with the fluctuation in methane production. A period of high influent COD was followed by a rise in methane production in all three AnMBRs.

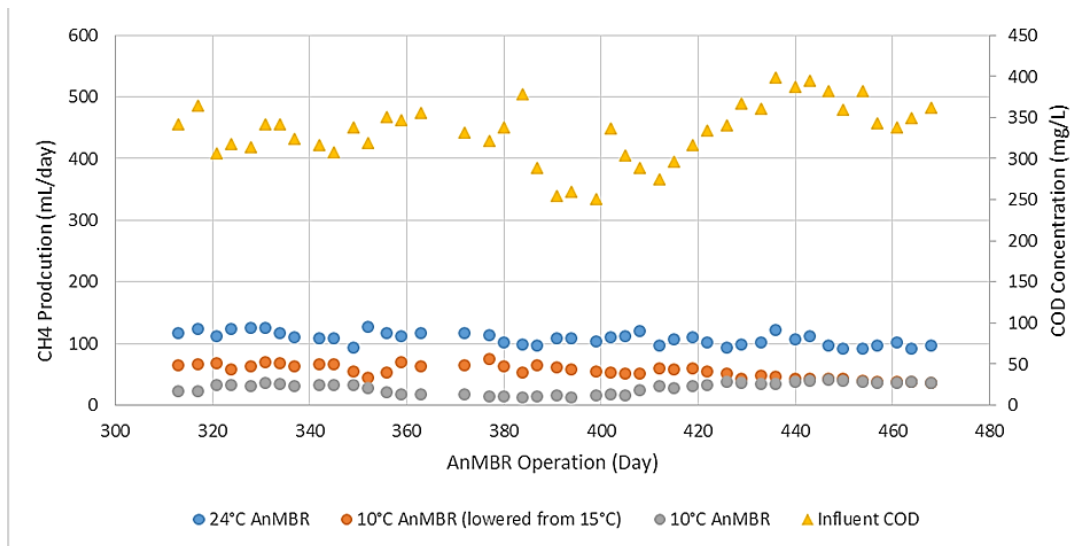


Figure 15 Phase 2 Methane Production Results

Table 13 summarizes the average steady state methane productions in mL/d at the three different temperatures. It can be observed that the 24°C AnMBR had the highest and most consistent methane production, as reflected in the standard deviation. Both the 10°C AnMBRs had lower methane production. The observation was consistent with the COD cumulative analysis, i.e. as temperature decreased, the fraction of COD converted to CH₄ decreased.

Table 13 Phase 2 Steady State Methane Productions

	Average Methane Production (mL/d)	Percent Change from Control
24°C	102 ± 8	N/A
10°C ¹	49 ± 9	52.0% Decrease
10°C	28 ± 10	72.5% Decrease

Notes:

1. Previously operated at 15°C during Phase 1 of the study.

4.4 Phase 3 AnMBR Performance

Phase 3 testing was conducted from Day 468 to Day 576. During this phase, three operations were run simultaneously with the 24°C AnMBR operated as control with no change from Phase 2, one 10°C AnMBR operated with no change from Phase 2, and one 10°C AnMBR dosed with PAC at 2 g/L. **Figure 16** presents the effluent COD of each AnMBR vs influent COD throughout Phase 3. From **Figure 16** it can be seen that the influent COD changed throughout this phase and this had an impact on all three effluents as exhibited in the corresponding pattern of COD concentrations. Further, it can be seen that even though PAC addition to the 10°C AnMBR started from Day 468, the effects of PAC on the biological performance of the AnMBR were not observed until approximately Day 520. It therefore suggests that steady state may have been established around Day 520.

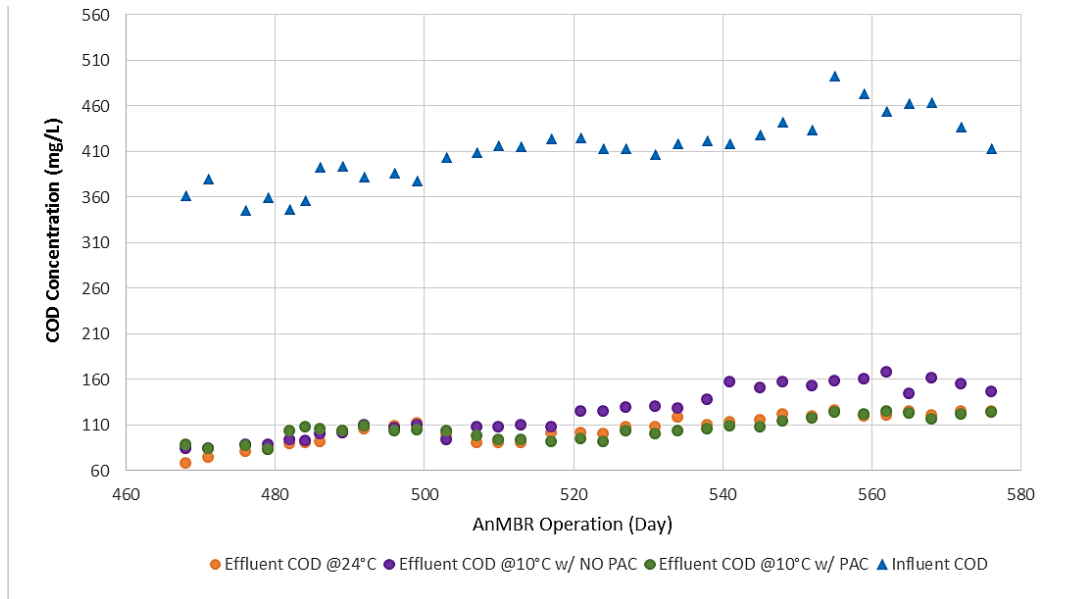


Figure 16 Phase 3 Effluent COD vs Influent COD Results

Table 14 summarizes the average COD removals and permeate CODs from the three AnMBRs after steady state was established. The 24°C AnMBR had the highest removal rate, at 74.6% corresponding to an average permeate COD of 104.8 mg/L. The 10°C AnMBR with PAC addition had the second highest average COD removal, at 74.5% and the 10°C AnMBR without PAC had the lowest COD removal, at 70.2% corresponding to a permeate COD of 123.4 mg/L.

Table 14 Phase 3 Summary of COD removals and permeate COD concentrations

	Average COD Removal	% Change from Control	Permeate COD (mg/L)
24°C	74.6 ± 2.6 %	N/A	104.8 ± 15.6
10°C	70.2 ± 4.4 %	5.9% Decrease	123.4 ± 26.4
10°C ¹	74.5 ± 2.2 %	0.1% Decrease	104.9 ± 11.8

Notes:

1. Psychrophilic AnMBR with 2g/L PAC addition.

To statistically compare the removal efficiencies of the three AnMBRs, a one-way analysis of variance (ANOVA) was completed on the average COD removal efficiencies. Results from the analysis are shown below in **Figure 17**. The null hypothesis was that all three average removal efficiencies were equal. It can be seen from the ANOVA summary that $F (18.76) > F \text{ crit} (3.09)$, therefore the null hypothesis was rejected. It was therefore concluded that the average COD removal efficiencies of the three AnMBRs were not all equal and at least one of the average removal efficiencies was different. Overall, the 24°C operation had the highest average COD removal, followed by the 10°C AnMBR operation with PAC addition. The 10°C AnMBR with no PAC addition had the lowest COD removal, which agrees with the findings from literature review that AnMBR performance declines with lowered operating temperatures due to decreased microbial activity inside the bioreactor (Chu et al., 2005; Ho and Sung, 2010).

SUMMARY						
<i>Groups</i>	<i>Count</i>	<i>Sum</i>	<i>Average</i>	<i>Variance</i>		
Column 1	33	2460.85	74.57	7.09		
Column 2	33	2317.72	70.23	20.01		
Column 3	33	2456.92	74.45	5.11		
ANOVA						
<i>Source of Variation</i>	<i>SS</i>	<i>df</i>	<i>MS</i>	<i>F</i>	<i>P-value</i>	<i>F crit</i>
Between Groups	402.85	2	201.42	18.76	0.00	3.09
Within Groups	1030.52	96	10.73			
Total	1433.36	98				

Figure 17 ANOVA Summary on Phase 3 Average COD Removal Efficiencies

To further compare the average removal efficiencies of all three operations, a Tukey’s test was applied simultaneously to all three pairwise comparisons: 24°C vs 10°C with PAC, 24°C vs 10°C, and 10°C vs 10°C with PAC. Results from the Tukey’s test are shown below in **Figure 18**.

q(24°C, 10°C PAC)	=	0.21							
df	=	96							
qCritical (from Studentized Range)	=	3.37							
q(24°C, 10°C PAC) < qCritical	The difference between the two means is NOT significant at a significance level of 0.05.								
q(24°C,10°C NO PAC)	=	0.40							
df	=	96							
qCritical (from Studentized Range)	=	3.37							
q(24°C,10°C NO PAC) < qCritical	The difference between the two means is NOT significant at a significance level of 0.05.								
q(10°C NO PAC,10°C PAC)	=	0.39							
df	=	96							
qCritical (from Studentized Range)	=	3.37							
q(10°C NO PAC,10°C PAC) < qCritical	The difference between the two means is NOT significant at a significance level of 0.05.								

Figure 18 Tukey Test Summary on Phase 3 Average COD Removal Efficiencies

The Tukey's test shows that at a significance level of 0.05, the average COD removal efficiencies between the 24°C and 10°C with PAC AnMBRs were not significantly different; the average COD removal efficiencies between the 24°C and 10°C AnMBRs were not significantly different; and the average COD removal efficiencies between the 10°C and 10°C with PAC AnMBRs were not significantly different. The removal efficiency of the 24°C AnMBR appeared to have deteriorated in this phase as compared to the other phases (74.6% in this phase compared to 80.2% in Phase 2 and 78.3% in Phase 1), which may have been responsible for the inability to differentiate between the three operations. Other indicators of performance subsequently presented in this section suggest that there were differences between the AnMBRs and hence the COD data may not have been the most indicative parameter of the biological performance of the AnMBRs. The detailed biological performance comparison between psychrophilic AnMBRs with and without PAC will be subsequently demonstrated in the COD fractionation analysis.

COD mass balance was conducted using the following equation:

$$\text{COD}_{\text{feed}} = \text{COD}_{\text{mass out}} + \text{accumulation, where}$$

$$\text{COD}_{\text{mass out}} = \text{COD}_{\text{WAS}} + \text{COD}_{\text{SO}_4} + \text{COD}_{\text{perm}} + \text{COD}_{\text{CH}_4}$$

The cumulative mass of all COD-bearing streams exiting the AnMBR plus the accumulation in the AnMBR for the 24°C operation were plotted versus time in **Figure 19** along with the mass of COD entering the MBR to assess the quality of the data by examining the mass balance closure.

In **Figure 19**, COD mass is represented on the y-axis. Therefore, the following interpretation applies to the figure:

$\text{COD}_{\text{feed}} = y(\text{feed})$, dark blue line

$\text{COD}_{\text{mass out} + \text{accumulation}} = y(\text{mass out} + \text{accumulation})$, orange line

$\text{COD}_{\text{WAS}} = y(\text{WAS})$, green line

$\text{COD}_{\text{SO}_4} = y(\text{SO}_4)$, purple line

$\text{COD}_{\text{perm}} = y(\text{perm})$, red line

$\text{COD}_{\text{CH}_4} = y(\text{CH}_4)$, light blue line

The approach used for the Phase 1 COD cumulative mass balance described in Section 4.2 was applied to Phase 3 COD data to form the analysis in this section. As seen in **Figure 19**, the COD streams exiting the MBR included sulfate reduction, permeate, waste activated sludge (WAS), and methane (CH₄). The sum of all streams leaving the bioreactor plus the accumulation inside the bioreactor was slightly less than the COD entering the bioreactor, showing a good COD balance.

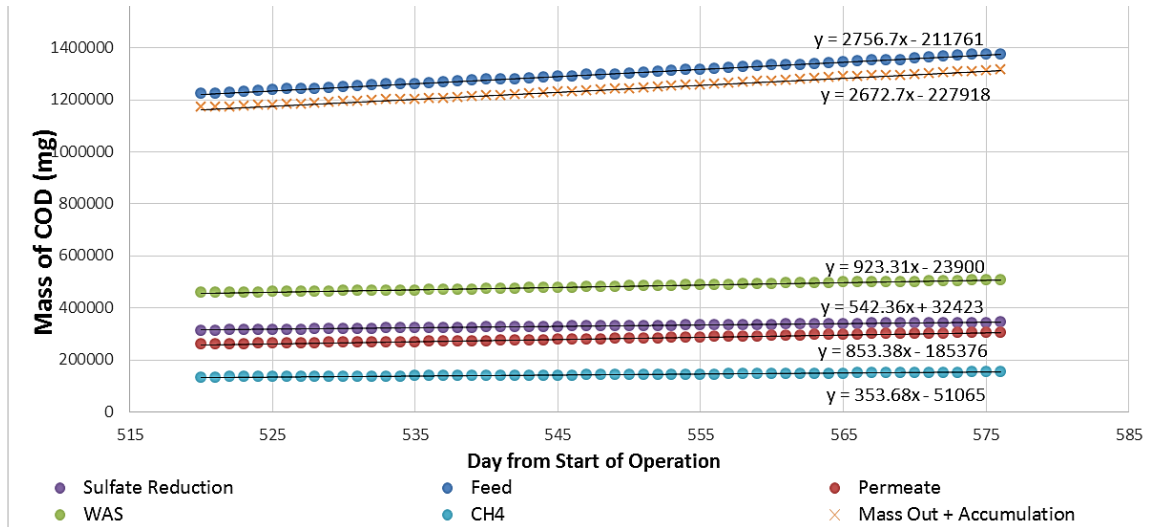


Figure 19 Phase 3 Steady State COD Mass Balance for the 24°C MBR

It can be seen in **Figure 19** that the line representing $COD_{\text{mass out} + \text{accumulation}}$ positions slightly below the line representing COD_{feed} . In a theoretical COD mass balance, the two lines would be overlapping each other with no deviation. In this study, deviation could be attributed to a less than perfect COD mass balance closure caused by several factors including experimental errors and the unmeasured methane saturated in permeate as a lost stream of COD. In future studies, it is recommended to develop a method to measure saturated methane in permeate.

Cumulative COD plots for the 10°C AnMBRs were generated using the same approach. The slope of each COD bearing stream was determined and used to come up with fractions of total COD going into the system. The fractions are presented in **Table 15**. It can be observed that compared to the 10°C AnMBR with no PAC addition, the 10°C operation with PAC addition had a higher f_{CH_4} and a lower f_{perm} . This observation suggests that adding PAC to the 10°C AnMBR increased the fraction of COD converted to CH_4 and decreased the fraction of COD used in removing organics as reflected in f_{perm} .

Table 15 COD Fractions of All COD Bearing Streams during Phase 3

	24°C	10°C	10°C ¹
f_{WAS}	33.5%	39.7%	36.0%
f_{PERM}	31.0%	50.1%	34.1%
f_{CH_4}	12.8%	11.3%	14.7%
f_{SO_4}	19.7%	20.5%	18.7%
$f_{\text{mass out+accum}}$	97.0%	124.5%	107.4%

Notes:

1. Psychrophilic AnMBR with 2g/L PAC addition.

The addition of PAC as a biofilm carrier potentially served as a biomass retention mechanism that allowed additional biodegradation not accomplished by the suspended biomass. In the AnMBRs without biofilm carriers, a portion of the suspended biomass would leave the AnMBRs every time the activated sludge was wasted. By retaining a portion of the active biomass inside the AnMBR, better biological performance was achieved as a possible outcome. Another possible explanation of the observed performance improvement was that a portion of the soluble COD inside the bioreactor was adsorbed onto PAC instead of passing through the membrane. As a result, a lower soluble COD was observed in the permeate.

VFA data were collected to compare the biological performance of each AnMBR in Phase 3 and the COD equivalences of the combined VFAs are presented in **Figure 20**. Similarly, the VFA-COD concentration in the influent stream is plotted in the same graph to show the relative concentrations of VFA entering each AnMBR.

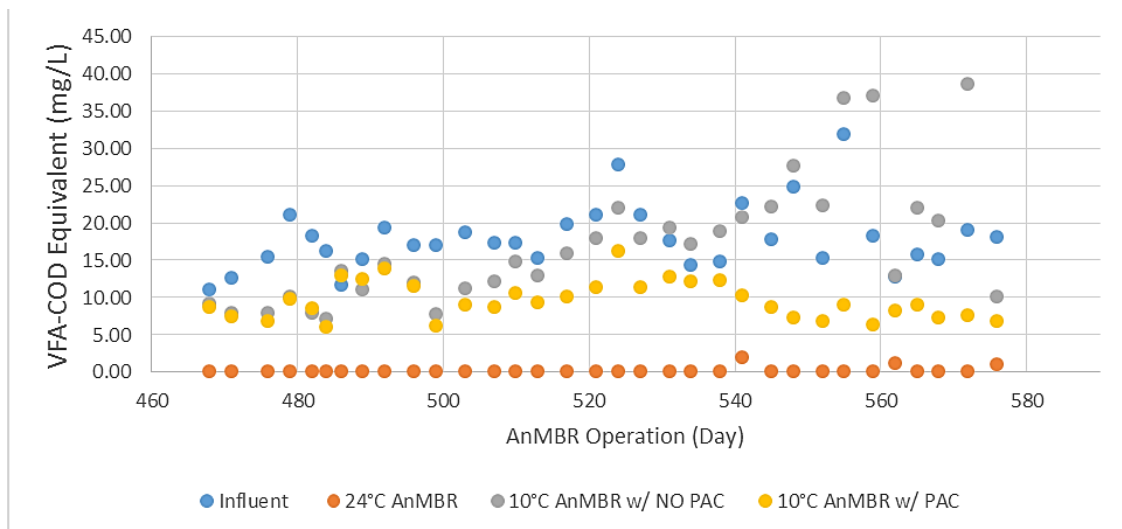


Figure 20 Phase 3 Influent vs Effluent VFA-COD

Figure 20 shows little accumulation of VFA in the 24°C AnMBR. The only two data points indicating VFA-COD were deemed to be not significant enough to suggest any VFA accumulation. The 10°C AnMBR with no PAC addition and the 10°C AnMBR with PAC addition both started with similar concentrations of VFA-COD at the start of Phase 3. After Day 510, the two AnMBRs started behaving differently. The 10°C AnMBR with no PAC addition continued to show high concentrations of VFA-COD and eventually reaching a maximum concentration of close to 40 mg/L around Day 580. This observation suggests VFA accumulation due to the imbalance between VFA production and utilization. On the other hand, the concentration of VFA-COD inside the 10°C AnMBR with PAC addition remained relatively steady at around 10 mg/L. VFA accumulation inside the 10°C AnMBR with PAC addition seemed to have been under control due to the improved performance of biological activities inside the bioreactor. This was consistent with the increased methane production in this AnMBR as compared to the AnMBR without PAC.

Table 16 summarizes the average steady state VFA-COD concentrations for the three different operations. The average VFA-COD concentrations at steady state show that the 10°C AnMBR with no PAC addition had the highest accumulation of acids, confirming the observation from **Figure 20**. Large standard deviations in the VFA-COD concentrations inside the AnMBRs could be attributed to the large fluctuations in influent VFA concentrations.

Table 16 Phase 3 Steady State VFA-COD Concentrations

	Average VFA-COD Concentration (mg/L)	Percent Change from Control
24°C	0.2 ± 0.5	N/A
10°C	21.3 ± 7.8	105.5% Increase
10°C ¹	9.6 ± 2.4	47.0% Increase

Notes:

1. Psychrophilic AnMBR with 2g/L PAC addition.

Methane production data were collected during Phase 3 and presented in **Figure 21**. Steady state was determined to have been established around Day 510. It can be observed that the overall methane production had an increasing trend for all three AnMBRs, corresponding to the increasing trend of influent COD. A period of high influent COD was followed by a rise in methane production in all three AnMBRs.

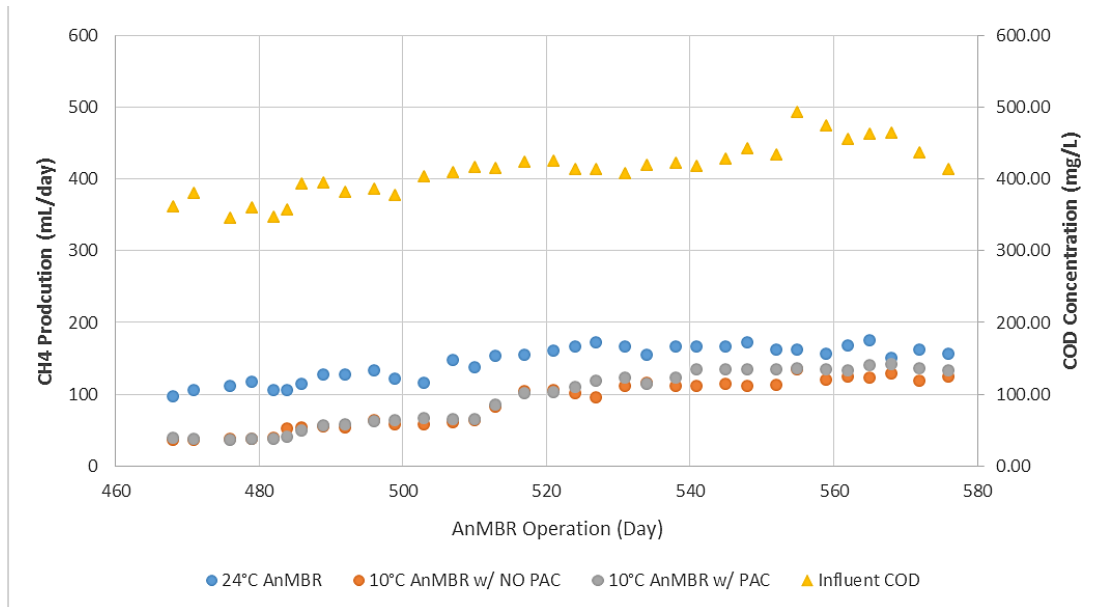


Figure 21 Phase 3 Methane Production Results

Table 17 summarizes the average steady state methane productions in mL/d for the three different operations. It can be observed that the 24°C AnMBR had the highest methane production throughout Phase 3, at an average production of 161 ± 8 mL/d. The 10°C AnMBR with no PAC addition had the lowest average methane production of 110 ± 16 mL/d. At 10°C with PAC addition, methane production was observed to be 122 ± 20 mL/d, higher than the psychrophilic AnMBR without PAC only by 12%. Compared to the 24°C AnMBR, the 10°C AnMBR with no PAC addition produced 50% less methane and the 10°C AnMBR with PAC addition produced 38% less methane. The results show that even with PAC addition, methane production was not increased significantly under psychrophilic conditions.

Table 17 Phase 2 Steady State Methane Productions

	Average Methane Production (mL/d)	Percent Change from Control
24°C	161 ± 8	N/A
10°C	110 ± 16	31.68% Decrease
10°C ¹	122 ± 20	24.22% Decrease

Notes:

1. Psychrophilic AnMBR with 2g/L PAC addition.

4.5 Physical Performance of Membranes

Throughout the study, transmembrane pressure (TMP) was monitored to evaluate the impact of temperature on membrane fouling. The AnMBRs were operated at a constant flux while TMP was monitored. Membrane fouling is accompanied by as an increase in TMP under constant permeate flux, which is described in the following equation:

$$J = \frac{\Delta P}{\mu \times R_t} \text{ (Equation 2)}$$

where J is the permeate flux, μ is the viscosity of activated sludge, ΔP is the TMP, and R_t is the total hydraulic filtration resistance. This equation explains the theoretical expectation of the membrane's behavior exhibited through TMP. To maintain the permeate flux, as temperature lowers and viscosity of the activated sludge increases, TMP increases as well.

In this study, the membranes were operated in a relaxed mode with 8 minutes of permeation followed by 2 minutes of relaxation. The mechanisms used to control membrane fouling included gas sparging, citric acid backwashing, and recovery cleaning of the membranes. Recovery cleaning of the membranes was conducted at the start of the study as well as between the two different phases. Recovery cleaning consisted of sequentially soaking each membrane in citric acid at 2 g/L and NaOCl at 2g/L for 16 hours respectively. It was also observed that a

discontinuation of biogas sparging due to pump failure caused abrupt membrane fouling evidenced by a substantial increase in TMP. It was concluded that biogas sparging is a prerequisite to having an operational AnMBR system. While backflushing was necessary to reduce short-term reversible membrane fouling and practiced on a regular basis, chemical cleaning of the membrane was crucial to mitigating long-term irreversible fouling.

Flux was maintained constant throughout the experiment and hence an increase in TMP was interpreted to indicate membrane fouling. Phase 1 TMP data collection was conducted to explore the impacts of low temperature on the membrane performance. Phase 3 TMP data collection was collected to assess the potential mitigation of fouling as a measure of the effectiveness of using a biofilm carrier. TMP was monitored for a 12 day period for each AnMBR and data are presented in Sections 4.15 to 4.16.

This section presents the results of physical performance evaluated using TMP increases in each AnMBR during Phase 1. **Figure 22** presents the TMP responses that were observed in the three AnMBRs during a 12 day monitoring period in Phase 1. The initial TMP at the start of all three AnMBR operations was approximately -3447.38 N/m^2 (-0.5 PSI). From these Figures it can be observed that TMP increases only occurred in the 10°C and 15°C AnMBRs during the monitoring period. In the 10°C AnMBR, the TMP increased to -30336.9 N/m^2 (-4.4 PSI) in a 7 day period. From Day 7 to Day 9, while TMP stayed around -30336.9 N/m^2 (-4.4 PSI), the production of permeate from this AnMBR decreased drastically. In the 15°C AnMBR, the TMP increased to -30336.9 N/m^2 (-4.4) PSI in a 10 day period. From Day 10 to Day 11, while TMP stayed around -30336.9 N/m^2 (-4.4) PSI, the production of permeate from this AnMBR decreased drastically. The increase in TMP observed in both psychrophilic AnMBRs is possibly due to the fact that the membrane was experiencing major reversible fouling due to either foulant

buildup on the membrane surface or colloidal particles blocking membrane pores. At a psychrophilic temperatures of 10°C and 15°C, the mixed liquor inside the AnMBR increased in viscosity. As predicted by the TMP – Viscosity equation presented at the beginning of this section, to maintain a constant flux, with decreasing temperature the TMP increases. Upon observing a TMP increase, permeate backflushing was applied to the 10°C and 15°C AnMBRs to reverse short term fouling. Applying backflushing was effective in restoring TMP to near the initial TMP at -3447.38 N/m^2 (-0.5 PSI), which could not be maintained for over 15 days however. This suggests that the initial performance of virgin membrane could not be replicated at psychrophilic temperatures with backflushing alone.

The first plot in **Figure 22** indicates that there were no TMP increases in the 24°C AnMBR over a 12 day period. The interval leading to the high fouling event was shorter for the 10°C AnMBR compared to the 15°C AnMBR. The same TMP increase behaviors were consistently observed throughout Phase 1 operation. The TMP increases in the 10°C and 15°C AnMBRs suggest increased membrane fouling due to lowered temperatures. The different times it took to reach reversible fouling in the 10°C and 15°C AnMBRs could be used as an additional indicator of membrane fouling potential at low temperatures.

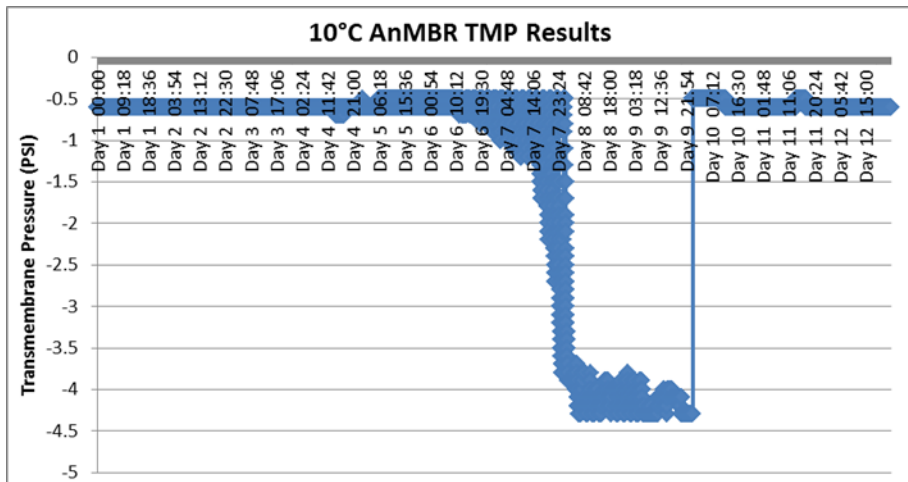
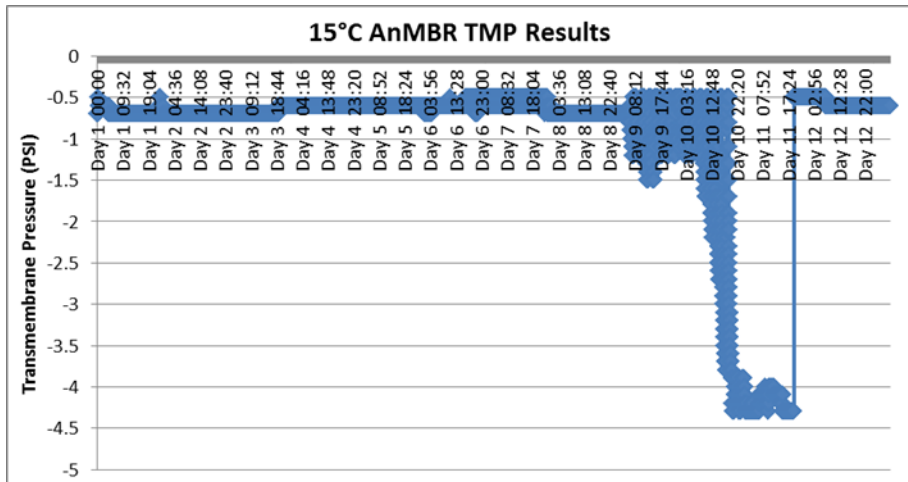
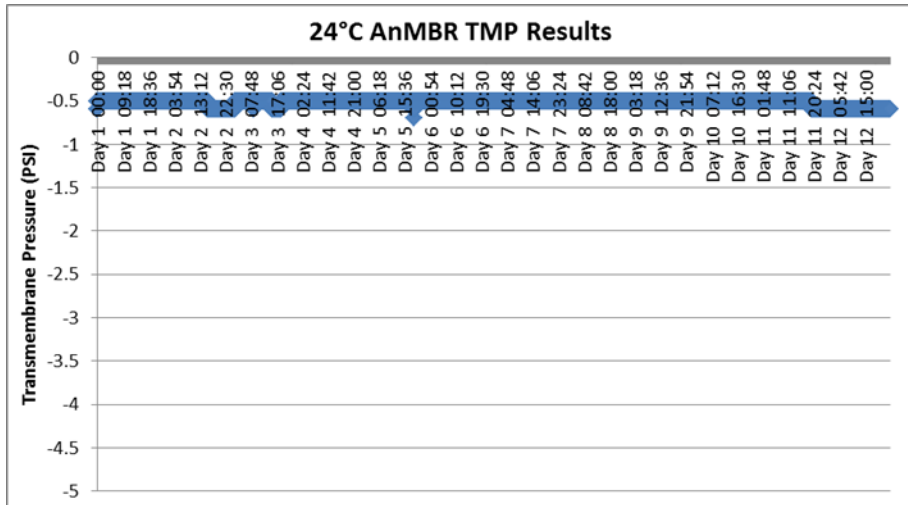


Figure 22 TMP Results from the 24°C, 15°C, and 10°C AnMBRs during Phase 1

To investigate the effects of biofilm carriers on the physical performance of membranes at psychrophilic temperatures, TMP continued to be monitored throughout Phase 3 of the study.

Figure 23 shows the TMP responses that were observed in the two psychrophilic AnMBRs (with and without PAC addition) during a 12 day monitoring period in Phase 3. The initial TMP at the start of both of the psychrophilic AnMBR operations was approximately -3447.38 N/m^2 (-0.5 PSI). TMP spikes were observed in both psychrophilic AnMBRs, suggesting increased membrane fouling due to lowered temperatures. In the 10°C AnMBR without PAC, the TMP increased to -30336.9 N/m^2 (-4.4 PSI) in a 7 day period. From Day 7 to Day 9, while TMP stayed around -30336.9 N/m^2 (-4.4 PSI), the production of permeate from this AnMBR decreased drastically. However, the psychrophilic AnMBR with PAC addition showed delayed TMP spikes in a 12 day period as compared to the AnMBR without PAC addition. The former value was approximately 11 days as compared to 7 days for the latter thereby suggesting improved permeability with PAC addition. It can also be concluded based on this study that even with PAC addition at the concentration of 2g/L, at psychrophilic temperatures, membrane's physical performance deteriorates. Backflushing has been shown to be effective in restoring the membrane's physical filtration performance. However, it was not successful to replicate the physical performance of virgin membranes at psychrophilic temperatures with backflushing.

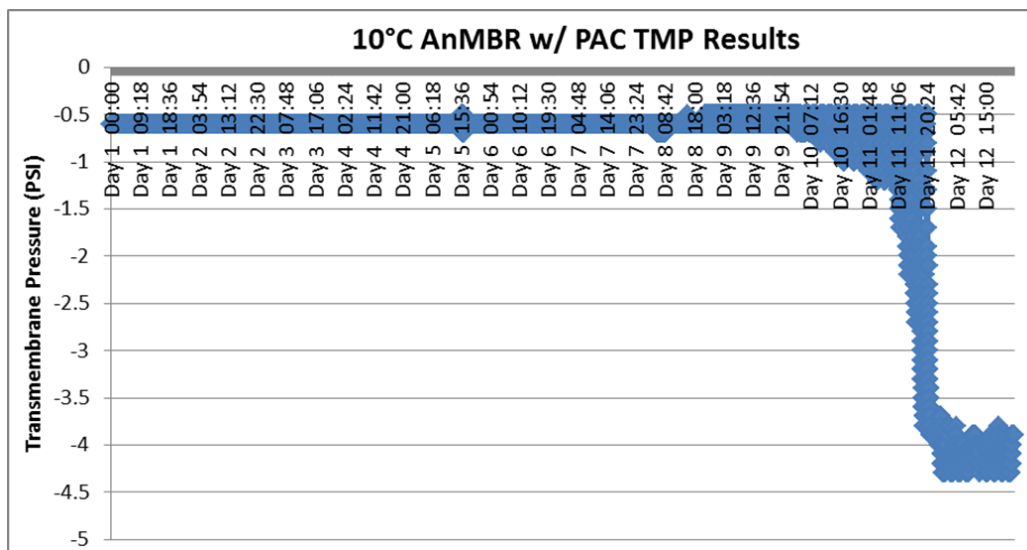
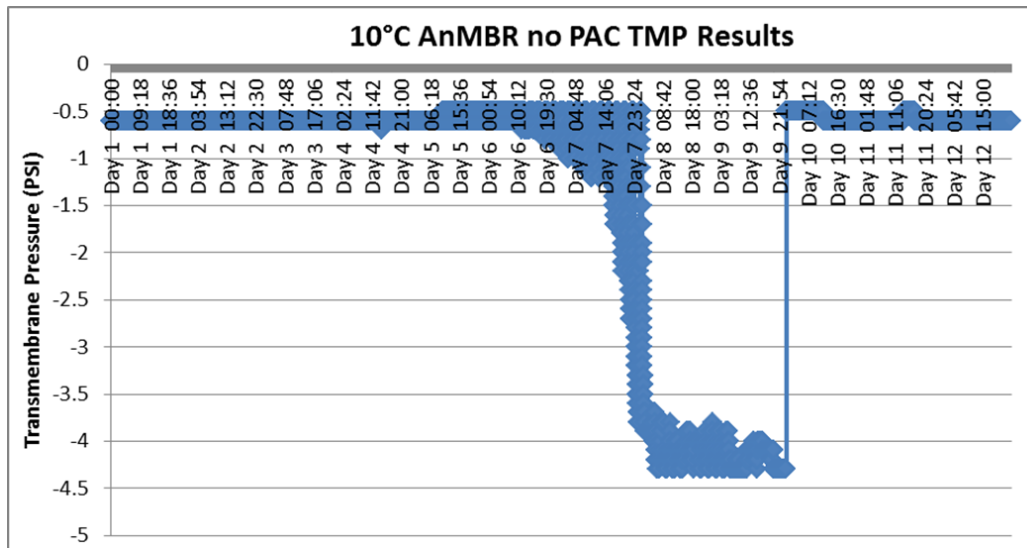


Figure 23 TMP Results from the 10°C AnMBRs during Phase 3

4.6 Summary

In this study, three lab-scale AnMBRs were operated to treat municipal sewage from the City of Waterloo over three phases. During the initial phase of operation, the AnMBRs were operated at 24°C, 15°C and 10°C respectively. TCOD, SCOD, TSS, VSS, VFA, biogas production, pH and TMP were regularly monitored to characterize the physical and biological performance of the AnMBRs. Compared to operation at 24°C, operation at 10°C resulted in decreased permeate

quality, lower biogas production, and unconsumed volatile fatty acids. There was no significant difference in performance of the AnMBRs operated at 24°C and 15°C.

During the second phase, one AnMBR was maintained at 24°C while two AnMBRs were operated at 10°C. The 24°C AnMBR had the highest COD removal and methane production. No accumulation of VFA was found in the 24°C AnMBR. As the previously 15°C AnMBR from Phase 1 was lowered to 10°C in Phase 2, its effluent quality decreased and VFA accumulation was observed in the bioreactor. The 10°C operation consistently showed poor COD removal and VFA accumulation compared to the other two AnMBRs.

In the final phase of the study, Powdered Activated Carbon (PAC) was added to one of the AnMBRs operated at 10°C to achieve a concentration of 2 g/L as a biofilm carrier. After 90 days of operation, the previously accumulated VFAs in this AnMBR declined in concentration, while the VFAs in the AnMBR without PAC were consistently elevated. In contrast to Phase 2, the psychrophilic AnMBR with PAC showed delayed TMP spikes in a 12 day period, suggesting improved permeability. However, methane production was not increased due to the addition of PAC in the psychrophilic AnMBR.

The following conclusions were made based on observations during the study:

- The 24°C AnMBR had higher COD removal and higher methane production than both the psychrophilic AnMBRs, even after PAC addition.
- Adding PAC to the psychrophilic AnMBR improved effluent quality as demonstrated in the increased COD removal. This could be due to the adsorption of soluble COD onto the PAC as well as the increased biomass retention via PAC.
- PAC addition helped stop VFA accumulation in one of the psychrophilic AnMBRs.

- Throughout the study, all three AnMBRs had lower methane production than theoretical reported values calculated assuming 350 L of methane was generated per kg of COD removed. This could be due to the presence of high concentrations of sulfate in the feed and dissolved methane in permeate.
- PAC addition delayed TMP spikes in a psychrophilic AnMBR over a 12 day period.
- Membrane fouling was successfully managed using biogas sparging and permeate backflushing.

Chapter 5: Conclusions and Recommendations

5.1 Conclusions

The objectives of this research were to evaluate the biological performance of AnMBRs under psychrophilic conditions, to investigate the fouling behavior of the membranes in AnMBRs under psychrophilic conditions, and to explore mitigation strategies to improve AnMBR performance at psychrophilic temperatures. Through operating three lab scale AnMBRs over three phases, biological and physical performances of each AnMBR were measured against parameters including permeate quality, biogas production, VFA accumulation, and TMP. A few conclusions can be drawn from the study. In terms of the biological performance of AnMBRs, compared to the 24°C operation, operation at 10°C was observed to have decreased permeate quality, lower biogas production, and unconsumed VFAs. Specifically, the 10°C AnMBR was observed have a 10.9% decrease in COD removal, a 65.8% decrease in methane production, and a 98% increase in unconsumed VFA when compared to the control AnMBR at 24°C. However, there was no significant difference in the performances of the 24°C and 15°C AnMBRs. VFA accumulation in the psychrophilic AnMBR with PAC addition decreased. VFAs in the psychrophilic AnMBR without PAC were consistently elevated. Compared to the control AnMBR, a 105.5% increase in unconsumed VFA was observed in the psychrophilic AnMBR without PAC addition was observed, whereas only a 47.0% increase was observed in the psychrophilic AnMBR with PAC addition.

In terms of the physical performance of each AnMBR, TMP spikes were observed in the psychrophilic AnMBRs, suggesting increased membrane fouling due to lowered temperatures. It was also observed that in the final phase of the study, the psychrophilic AnMBR with PAC

addition showed delayed TMP spikes in a 12 day period as compared to the AnMBR without PAC addition. TMP results suggest that improved permeability can be achieved through PAC addition.

5.2 Recommendations

A few recommendations can be made on future research in the area of the evaluation of AnMBR performance at psychrophilic temperatures and mitigation strategies for fouling:

- Investigate PAC addition to psychrophilic AnMBRs at different concentrations to find the optimal concentration;
- Explore different biofilm carrier options, including but are not limited to PAC, GAC, plastic beads, plastic re-granulates, and plant-based carriers;
- Vary operational conditions such as SRT and HRT to optimize for operation under psychrophilic conditions;
- Conduct process simulation through software such as BioWin to predict AnMBR performance at psychrophilic temperatures; and
- Scale up the operations through a pilot study.

References

- Abu-Obaid, S. (2018). Characterization of Fouling of Tertiary Membranes Treating Secondary Effluent of Domestic Wastewater. Master of Applied Science Thesis. Civil Engineering, University of Waterloo.
- Bandara, W. M.; Satoh, H.; Sasakawa, M.; Nakahara, Y.; Takahashi, M.; & Okabe, S. (2011). Removal of residual dissolved methane gas in an upflow anaerobic sludge blanket reactor treating low-strength wastewater at low temperature with degassing membrane Water Res. 2011, 45 (11) 3533– 3540
- Bandara, W. M.; Kindaichi, T.; Satoh, H.; Sasakawa, M.; Nakahara, Y.; Takahashi, M.; & Okabe, S. (2012). Anaerobic treatment of municipal wastewater at ambient temperature: Analysis of archaeal community structure and recovery of dissolved methane Water Res. 2012, 46 (17) 5756– 5764.
- Chu, L.B., Yang, F.L. & Zhang, X.W. (2005). Anaerobic treatment of domestic wastewater in a membrane-coupled expanded granular sludge bed (EGSB) reactor under moderate to low temperature. Process Biochemistry 40(3-4), 1063-1070.
- Cookney, J.; Cartmell, E.; Jefferson, B.; & McAdam, E. (2012). Recovery of methane from anaerobic process effluent using poly-di-methyl-siloxane membrane contactors Water Sci. Technol. 2012, 65 (4) 604– 610.
- Giménez, J.; Robles, A.; Carretero, L.; Durán, F.; Ruano, M.; Gatti, M.; Ribes, J.; Ferrer, J.; & Seco, A. (2011). Experimental study of the anaerobic urban wastewater treatment in a submerged hollow-fibre membrane bioreactor at pilot scale Bioresour. Technol. 2011, 102 (19) 8799– 8806
- Grady Jr, C. P. L., Daigger, G. T., Love, N. G., & Filipe, C. D. M. (2011). Biological Wastewater Treatment, Third Edition. CRC Press. ISBN 9780849396793 - CAT# 9679
- Hartley, K. & Lant, P. (2006). Eliminating non-renewable CO₂ emissions from sewage treatment: An anaerobic migrating bed reactor pilot plant study Biotechnol. Bioeng. 2006, 95 (3) 384– 398.
- Hejnic, J., Dolejs P., Kouba V., Prudilova A., Widiayuningrum P., & Bartacek J. (2016). Anaerobic Treatment of Wastewater in Colder Climates Using UASB Reactor and Anaerobic Membrane Bioreactor. Environmental Engineering Science. Vol. 33, No. 11.
- Hai, F.I., Yamamoto, K. & Lee, C-H. (2013). Membrane Biological Reactors. IWA Publishing, Nov. 1, 2013. P 363.
- Ho, J. & Sung, S. (2010). Methanogenic activities in anaerobic membrane bioreactors (AnMBR) treating synthetic municipal wastewater. Bioresource Technology 101(7), 2191-2196.

- Hu, A. & Stuckey, D. (2007). Activated Carbon Addition to a Submerged Anaerobic Membrane Bioreactor: Effect on Performance, Transmembrane Pressure, and Flux. *Journal of Environmental Engineering* 133(1). DOI: 10.1061/(ASCE)0733-9372(2007)133:1(73).
- Kobayashi, H.; Stenstrom, M.; & Mah, R. (1983). Treatment of low strength domestic wastewater using the anaerobic filter *Water Res.* 1983, 17 (8) 903– 909.
- Li, H. & Chen, V. (2010). Membrane Fouling and Cleaning in Food and Bioprocessing. *Membrane Technology*. 2010, Pages 213-254.
- Liu, Z., Yin, H., Dang, Z., & Liu, Y. (2013). Dissolved Methane: A Hurdle for Anaerobic Treatment of Municipal Wastewater. *Environ. Sci. Technol.* 2014, 48, 889–890.
- Matsuura, N.; Hatamoto, M.; Sumino, H.; Syutsubo, K.; Yamaguchi, T.; & Ohashi, A. (2015). Recovery and biological oxidation of dissolved methane in effluent from UASB treatment of municipal sewage using a two-stage closed downflow hanging sponge system *J. Environ. Manage.* 2015, 151, 200– 209
- Martinez-Sosa, D., Helmreich, B., Netter, T., Paris, S., Bischof, F. & Horn, H. (2011). Anaerobic Submerged Membrane Bioreactor (AnSMBR) for Municipal Wastewater Treatment under Mesophilic and Psychrophilic Temperature Conditions. *Bioresource. Technology*. 2011, 102, 10377–10385.
- Park, H., Choo, K-H., & Lee, C-H. (1999). *Separation Science and Technology*. Volume 34, 1999 - Issue 14.
- Smith, A. L., Skerlos, S. J. & Raskin, L. (2013). Psychrophilic anaerobic membrane bioreactor treatment of domestic wastewater. *Water Res.* 2013, 47 (4), 1655–1665.
- Smith, A. L. (2014). Low-Temperature Anaerobic Membrane Bioreactor for Energy Recovery from Domestic Wastewater. PhD Dissertation. *Environmental Engineering*, University of Michigan.
- Smith, A.L., Skerlos, S.J. & Raskin, L. (2015). Anaerobic Membrane Bioreactor Treatment of Domestic Wastewater at Psychrophilic Temperatures Ranging from 15 °C to 3 °C. *Environ. Sci. Water Res. Technol.* 2015, 1, 56–64.
- Souza, C.; Chernicharo, C.; & Aquino, S. (2011). Quantification of dissolved methane in UASB reactors treating domestic wastewater under different operating conditions *Water Sci. Technol.* 2011, 64 (11) 2259– 2264.
- Stuckey, D. (2010). Anaerobic Membrane Reactors. *Environmental Anaerobic Technology*. DOI: 10.1142/9781848165434_0007.2

Vela, J.D., Stadler, L.B., Martin, K.J., Raskin, L., Bott, C.B., & Love, N.G. (2015). Prospects for Biological Nitrogen Removal from Anaerobic Effluents during Mainstream Wastewater Treatment. *Environmental Science & Technology Letters*. 2015 2 (9), 234-244.

Appendix A – Phase 1 Data for All AnMBRs

Phase 1 COD Data

Day	Influent COD	Effluent COD @24°C	COD Removal @24°C	Effluent COD @15°C	COD Removal @15°C	Effluent COD @10°C	COD Removal @10°C
1	316.58	65.13	79.43	39.09	87.65	39.49	87.53
5	412.42	55.42	86.56	41.07	90.04	40.47	90.19
8	469.62	63.20	86.54	40.08	91.47	41.46	91.17
13	434.12	60.89	85.97	50.73	88.31	51.32	88.18
17	332.36	66.53	79.98	64.14	80.70	74.99	77.44
21	535.88	66.40	87.61	50.61	90.55	54.70	89.79
24	322.49	47.57	85.25	40.47	87.45	39.49	87.75
27	541.60	50.34	90.71	45.70	91.56	47.87	91.16
30	412.23	52.70	87.22	50.93	87.65	56.25	86.35
34	314.61	68.43	78.25	42.84	86.38	40.08	87.26
37	319.54	68.09	78.69	41.85	86.90	39.69	87.58
40	319.54	70.12	78.06	49.46	84.52	48.99	84.67
44	331.57	66.40	79.97	59.60	82.02	61.38	81.49
50	303.96	70.43	76.83	59.60	80.39	58.03	80.91
53	303.96	77.46	74.51	63.32	79.17	58.62	80.71
57	431.55	71.83	83.36	68.28	84.18	59.41	86.23
61	431.55	63.94	85.18	73.91	82.87	66.62	84.56
64	488.95	58.03	88.13	78.14	84.02	72.03	85.27
66	441.42	57.63	86.94	78.14	82.30	68.48	84.49
69	358.19	58.22	83.75	68.28	80.94	67.69	81.10
71	342.81	59.41	82.67	69.86	79.62	60.20	82.44
73	343.40	67.49	80.35	68.48	80.06	69.86	79.66
77	309.08	61.77	80.01	67.10	78.29	64.53	79.12
80	313.62	60.00	80.87	68.28	78.23	69.07	77.98
85	322.89	59.41	81.60	69.07	78.61	60.98	81.11
88	306.13	61.97	79.76	62.96	79.43	61.77	79.82
92	305.73	59.41	80.57	69.07	77.41	60.98	80.05
96	305.73	72.93	76.15	73.35	76.01	69.32	77.33
99	343.40	83.07	75.81	76.56	77.71	75.58	77.99
102	343.40	84.05	75.52	80.71	76.50	86.33	74.86

105	293.50	97.08	66.92	84.85	71.09	97.08	66.92
113	412.62	74.79	81.87	78.54	80.97	73.80	82.11
118	359.37	35.35	90.16	79.52	77.87	71.63	80.07
121	366.08	43.83	88.03	77.55	78.82	78.73	78.49
125	391.72	57.63	85.29	86.03	78.04	95.70	75.57
127	404.93	74.40	81.63	79.52	80.36	90.96	77.54
131	404.93	78.25	80.68	81.69	79.83	90.96	77.54
135	408.09	82.09	79.88	83.86	79.45	90.96	77.71
140	418.74	94.51	77.43	92.34	77.95	91.75	78.09
144	418.74	82.94	80.19	87.43	79.12	92.98	77.80
149	447.33	68.48	84.69	81.30	81.83	94.51	78.87
152	447.33	71.64	83.99	75.78	83.06	103.39	76.89
155	428.60	74.79	82.55	70.25	83.61	112.26	73.81
158	428.60	77.07	82.02	73.13	82.94	113.44	73.53
162	419.52	80.11	80.90	76.96	81.66	115.02	72.58
166	419.52	87.55	79.13	78.09	81.39	113.90	72.85
169	459.95	93.13	79.75	78.93	82.84	113.05	75.42
173	459.95	94.18	79.52	86.91	81.10	122.25	73.42
178	459.95	95.50	79.24	96.88	78.94	133.76	70.92
183	386.59	102.60	73.46	98.06	74.63	139.67	63.87
186	386.59	91.22	76.40	111.87	71.06	145.39	62.39
189	526.61	100.34	80.95	125.67	76.14	151.11	71.31
193	526.61	90.90	82.74	107.98	79.50	133.87	74.58
196	489.73	87.30	82.17	94.71	80.66	120.94	75.30
200	367.66	87.02	76.33	104.18	71.66	146.38	60.19
203	367.66	90.57	75.37	99.84	72.85	140.86	61.69
209	370.61	96.48	73.97	91.15	75.41	129.81	64.97
212	333.14	90.96	72.70	100.82	69.74	126.46	62.04
215	333.14	91.66	72.49	99.58	70.11	124.09	62.75
223	341.42	93.52	72.61	96.28	71.80	117.78	65.50
226	354.04	94.11	73.42	91.75	74.08	117.58	66.79
230	357.20	98.65	72.38	87.21	75.59	115.81	67.58
234	358.19	87.09	75.69	98.06	72.62	119.56	66.62

236	331.33	88.12	73.40	92.33	72.13	113.00	65.90
240	357.67	90.00	74.84	83.33	76.70	115.33	67.75
244	373.83	89.00	76.19	83.33	77.71	115.83	69.01
249	372.00	81.67	78.05	85.17	77.11	124.17	66.62
253	372.00	77.67	79.12	79.50	78.63	121.75	67.27
255	365.17	75.67	79.28	76.67	79.01	119.33	67.32
260	400.17	75.67	81.09	66.67	83.34	131.67	67.10
265	354.50	78.33	77.90	77.17	78.23	122.83	65.35
269	389.50	79.17	79.67	81.50	79.08	119.33	69.36
274	377.83	72.33	80.86	85.67	77.33	116.00	69.30
278	377.83	72.58	80.79	75.59	79.99	117.92	68.79
282	316.33	72.83	76.98	65.50	79.29	119.83	62.12
287	317.83	65.33	79.44	67.67	78.71	120.30	62.15
292	376.67	84.83	77.48	79.00	79.03	121.00	67.88
296	317.50	78.50	75.28	90.00	71.65	114.50	63.94
301	327.50	80.17	75.52	90.00	72.52	121.83	62.80
305	349.50	100.83	71.15	94.67	72.91	126.83	63.71
310	341.50	103.33	69.74	94.67	72.28	107.67	68.47
Average	387.59	82.98	78.26	86.77	77.30	115.19	69.81
Min	293.50	35.35	66.92	65.50	69.74	71.63	60.19
Max	541.60	103.33	90.16	125.67	83.61	151.11	82.11
Standard Dev	59.78	13.44	4.52	11.75	3.88	17.44	5.79

Phase 1 COD ANOVA

COD Removal @15°C	COD Removal @10°C
71.09	66.92
80.97	82.11
77.87	80.07
78.82	78.49
78.04	75.57
80.36	77.54
79.83	77.54
79.45	77.71
77.95	78.09
79.12	77.80
81.83	78.87
83.06	76.89
83.61	73.81
82.94	73.53
81.66	72.58
81.39	72.85
82.84	75.42
81.10	73.42
78.94	70.92
74.63	63.87
71.06	62.39
76.14	71.31
79.50	74.58
80.66	75.30
71.66	60.19
72.85	61.69
75.41	64.97
69.74	62.04
70.11	62.75
71.80	65.50
74.08	66.79
75.59	67.58
72.62	66.62
72.13	65.90
76.70	67.75
77.71	69.01
77.11	66.62
78.63	67.27
79.01	67.32
83.34	67.10

Anova: Single Factor

SUMMARY

Groups	Count	Sum	Average	Variance
Column 1	51	3991.33	78.26	20.80
Column 2	51	3942.33	77.30	15.38
Column 3	51	3560.56	69.81	34.18

ANOVA

Source of Variation	SS	df	MS	F	P-value	F crit
Between Groups	2181.18	2.00	1090.59	46.51	0.00	3.06
Within Groups	3517.51	150.00	23.45			
Total	5698.69	152.00				

Conclusion: $F (46.51) > F \text{ crit } (3.06)$, therefore we reject the null hypothesis. The means of the three populations are not all equal. At least one of the means is different.

Pair (1,2) Mean Difference	0.960716379	SE(1,2)	0.678089231
Pair (1,3) Mean Difference	8.446551115	SE(1,3)	0.678089231
Pair (2,3) Mean Difference	7.485834735	SE(2,3)	0.678089231

q(24°C, 10°C)	=	12.46
df	=	150
qCritical (from Studentized Range)	=	3.31
q(24°C, 10°C) > qCritical	The difference between the two means is significant at a significance level of 0.05.	

q(24°C, 15°C)	=	1.42
df	=	150
qCritical (from Studentized Range)	=	3.31
q(24°C, 15°C) < qCritical	The difference between the two means is NOT significant at a significance level of 0.05.	

q(15°C, 10°C)	=	11.04
df	=	150
qCritical (from Studentized Range)	=	3.31
q(15°C, 10°C) > qCritical	The difference between the two means is significant at a significance level of 0.05.	

78.23	65.35
79.08	69.36
77.33	69.30
79.99	68.79
79.29	62.12
78.71	62.15
79.03	67.88
71.65	63.94
72.52	62.80
72.91	63.71
72.28	68.47

Phase 1 Methane Production Data

Day	Influent COD	24°C AnMBR	15°C AnMBR	10°C AnMBR
1	316.58	97.42	146.23	83.16
5	412.42	96.92	157.67	106.92
8	469.62	90.46	114.37	94.46
13	434.12	80.35	139.81	80.35
17	332.36	85.56	144.07	85.56
21	535.88	85.61	138.22	85.61
24	322.49	80.64	133.13	95.04
27	541.60	71.28	136.08	95.04
30	412.23	81.58	129.89	102.96
34	314.61	83.35	124.77	88.70
37	319.54	68.11	131.33	82.18
40	319.54	54.33	137.50	92.66
44	331.57	63.60	129.15	94.25
50	303.96	53.51	127.14	87.00
53	303.96	60.91	131.00	81.10
57	431.55	65.09	129.36	70.99
61	431.55	86.15	123.18	74.47
64	488.95	84.00	123.55	65.91
66	441.42	82.94	130.94	63.12
69	358.19	78.83	126.73	68.34
71	342.81	72.62	131.76	69.13
73	343.40	71.70	130.68	73.12
77	309.08	63.69	131.38	78.02
80	313.62	69.89	112.57	83.58
85	322.89	65.52	127.35	83.21
88	306.13	62.49	130.43	87.20
92	305.73	59.33	127.78	80.88
96	305.73	61.30	125.05	81.82
99	343.40	54.94	131.00	89.83
102	343.40	59.62	128.99	70.66
105	293.50	65.86	126.94	77.04
113	412.62	75.26	93.93	48.05
118	359.37	103.49	82.66	55.54
121	366.08	112.75	89.43	82.42
125	391.72	150.53	104.11	73.32
127	404.93	153.12	103.59	61.03
131	404.93	146.38	107.09	66.78
135	408.09	127.01	104.80	68.90
140	418.74	110.44	100.37	63.65
144	418.74	133.06	92.84	58.00
149	447.33	143.38	92.40	56.16
152	447.33	136.80	99.55	56.40
155	428.60	135.02	106.13	56.45
158	428.60	146.71	95.27	57.44
162	419.52	134.56	83.23	61.20
166	419.52	133.20	81.69	59.74

169	459.95	134.50	84.86	57.96
173	459.95	142.40	70.66	56.49
178	459.95	143.20	70.45	52.27
183	386.59	125.90	70.06	44.86
186	386.59	135.48	66.78	44.35
189	526.61	110.59	52.92	43.85
193	526.61	106.46	63.59	38.95
196	489.73	107.20	69.70	35.28
200	367.66	106.12	63.36	55.30
203	367.66	104.41	53.42	43.68
209	370.61	106.89	51.74	35.90
212	333.14	107.20	31.74	14.07
215	333.14	104.97	34.92	13.20
223	341.42	105.78	51.12	36.84
226	354.04	101.53	43.06	14.40
230	357.20	105.97	46.46	12.24
234	358.19	106.25	38.59	24.16
236	331.33	110.12	42.69	16.46
240	357.67	126.43	54.10	19.61
244	373.83	115.17	49.68	21.24
249	372.00	94.25	56.45	20.06
253	372.00	111.04	59.98	20.93
255	365.17	116.48	63.11	22.38
260	400.17	109.67	61.52	18.82
265	354.50	122.98	55.75	19.39
269	389.50	123.48	56.86	25.06
274	377.83	130.77	62.98	25.23
278	377.83	116.24	64.43	27.65
282	316.33	103.22	67.90	29.14
287	317.83	103.89	61.72	26.18
292	376.67	115.31	65.17	22.46
296	317.50	99.00	64.98	23.33
301	327.50	103.87	70.16	23.43
305	349.50	107.85	70.03	23.07
310	341.50	112.93	65.14	23.13

Average	380.56	117.35	70.98	39.87
Min	293.50	53.51	31.74	12.24
Max	541.60	153.12	157.67	106.92
Standard Dev	59.78	26.84	33.98	26.74

Phase 1 VFA Data

Day	Influent VFA-COD	24°C AnMBR	15°C AnMBR	10°C AnMBR
1	10.01	0.00	0.00	0.00
5	12.09	0.00	0.00	0.00
8	9.24	0.00	0.00	0.00
13	8.42	0.00	0.00	0.00
17	8.95	0.00	0.00	0.00
21	7.55	0.00	0.00	0.00
24	8.22	0.00	0.00	0.00
27	11.35	0.00	0.00	0.00
30	14.47	0.14	0.00	0.00
34	13.46	0.00	0.00	0.00
37	11.45	0.00	0.00	0.00
40	10.46	0.00	0.00	0.00
44	9.57	0.00	0.00	0.00
50	15.35	0.00	0.00	0.00
53	14.20	0.00	0.00	0.00
57	14.30	0.00	0.00	0.00
61	12.44	0.00	0.00	0.00
64	10.35	0.00	0.00	0.00
66	3.66	0.00	0.00	0.00
69	7.36	0.00	0.00	0.00
71	8.37	0.00	0.00	0.00
73	6.24	0.00	0.00	1.32
77	9.32	0.22	0.00	0.00
80	11.23	0.00	0.00	0.00
85	10.35	0.00	0.00	1.22
88	8.55	0.00	0.00	1.32
92	7.34	0.00	0.00	0.00
96	9.00	0.00	0.00	1.22
99	4.46	0.00	0.00	2.35
102	6.46	0.00	0.00	2.25
105	7.00	0.00	0.00	1.99
113	9.66	0.00	0.00	2.33
118	8.09	0.00	1.33	2.44
121	10.34	0.00	0.00	1.33
125	11.37	0.00	0.00	1.33
127	12.44	0.00	0.00	1.65
131	11.69	0.00	0.00	1.00
135	12.44	0.00	0.00	1.34
140	11.09	0.00	0.00	5.34
144	12.32	0.00	0.00	4.24
149	15.25	0.00	0.00	3.25
152	13.54	0.00	0.00	3.55
155	10.34	0.00	0.00	4.12
158	12.44	0.00	0.00	4.23
162	10.25	0.00	0.00	5.66
166	11.34	0.00	0.00	5.23

169	15.44	0.00	0.00	4.78
173	13.44	0.00	0.00	3.55
178	16.24	0.00	0.00	6.36
183	15.24	0.00	0.00	7.44
186	17.44	0.00	0.00	5.36
189	11.44	0.00	0.00	4.44
193	12.10	0.00	0.00	4.12
196	11.35	0.00	0.00	0.00
200	11.39	0.00	0.00	5.23
203	7.47	0.00	0.00	4.32
209	8.54	0.00	0.00	4.98
212	7.54	0.00	0.32	0.44
215	7.41	0.00	0.00	3.36
223	8.29	0.00	0.00	3.36
226	7.42	0.00	0.00	3.46
230	8.53	0.00	0.00	1.35
234	4.77	0.00	1.34	0.00
236	6.24	0.00	0.00	2.46
240	7.34	1.33	0.00	3.35
244	7.24	0.00	0.00	3.46
249	9.24	0.00	0.00	2.44
253	20.34	0.00	1.23	5.32
255	10.24	0.00	0.00	4.44
260	12.46	0.50	0.00	6.55
265	7.36	0.00	0.00	6.93
269	4.24	0.00	0.00	6.79
274	3.49	0.00	0.00	6.45
278	7.37	0.00	0.00	0.00
282	8.19	0.00	0.00	0.43
287	9.13	0.00	0.00	4.24
292	9.34	0.00	0.00	0.32
296	14.44	0.00	0.00	7.53
301	12.44	0.00	0.00	6.50
305	10.94	0.00	0.00	7.53
310	7.77	0.00	0.00	3.57

Average	10.19	0.04	0.12	3.96
Min	3.49	0.00	0.00	0.00
Max	20.34	1.33	1.34	7.53
Standard Dev	3.20	0.16	0.28	2.39

Appendix B – Phase 2 Data for All AnMBRs

Phase 2 COD Data

Day	Influent COD	Effluent COD @24°C	COD Removal @24°C	Effluent COD @10°C (lowered from 15°C)	COD Removal @10°C	Effluent COD @10°C	COD Removal @10°C
310	341.50	103.33	69.74	94.67	72.28	107.67	68.47
313	341.50	89.49	73.79	84.12	75.37	106.00	68.96
317	364.30	71.04	80.50	70.06	80.77	106.40	70.79
321	305.34	65.72	78.48	73.61	75.89	106.94	64.98
324	317.17	68.48	78.41	59.41	81.27	104.57	67.03
328	312.83	58.62	81.26	66.31	78.80	95.10	69.60
331	341.50	74.67	78.14	84.83	75.16	95.10	72.15
334	341.50	69.60	79.62	74.78	78.10	106.00	68.96
337	323.48	64.53	80.05	64.73	79.99	101.83	68.52
342	315.99	66.11	79.08	70.06	77.83	97.67	69.09
345	307.51	64.53	79.01	64.93	78.89	97.47	68.30
349	336.89	66.31	80.32	63.35	81.20	95.50	71.65
352	318.55	64.14	79.86	63.35	80.11	103.58	67.48
356	349.91	61.58	82.40	65.72	81.22	94.31	73.05
359	369.23	69.47	81.19	69.27	81.24	90.76	75.42
363	373.97	77.75	79.21	65.13	82.59	97.67	73.88
367	373.97	76.67	79.50	75.00	79.94	93.33	75.04
372	331.50	75.33	77.28	67.00	79.79	94.30	71.55
377	316.50	68.17	78.46	69.17	78.15	100.67	68.19
380	307.33	64.17	79.12	67.33	78.09	89.83	70.77
384	305.83	62.33	79.62	68.83	77.49	92.67	69.70
387	288.33	61.83	78.55	68.83	76.13	86.00	70.17
391	253.33	56.83	77.57	63.67	74.87	88.83	64.93
394	258.67	64.00	75.26	54.17	79.06	83.67	67.65
399	250.00	60.17	75.93	55.17	77.93	82.50	67.00
402	335.50	62.67	81.32	63.17	81.17	87.50	73.92
405	302.83	62.33	79.42	59.67	80.30	69.17	77.16
408	288.00	57.83	79.92	54.17	81.19	85.67	70.25
412	274.17	61.67	77.51	56.17	79.51	83.50	69.54
415	295.50	63.33	78.57	58.83	80.09	80.83	72.65
419	315.50	63.67	79.82	64.17	79.66	74.17	76.49
422	333.50	70.50	78.86	75.93	77.23	88.33	73.51
426	340.06	80.84	76.23	66.67	80.39	100.00	70.59
429	365.83	76.17	79.18	70.17	80.82	106.96	70.76
433	359.75	65.00	81.93	66.30	81.57	83.33	76.84
436	398.39	65.00	83.68	69.17	82.64	76.67	80.76
440	386.63	66.67	82.76	69.83	81.94	76.83	80.13
443	394.61	62.17	84.25	66.83	83.06	89.67	77.28
447	382.01	62.17	83.73	76.83	79.89	93.00	75.66
450	358.28	64.00	82.14	71.83	79.95	84.83	76.32
454	382.01	62.17	83.73	77.83	79.63	88.00	76.96
457	342.32	62.50	81.74	87.83	74.34	84.83	75.22
461	336.86	61.67	81.69	69.17	79.47	89.17	73.53
464	349.04	66.67	80.90	84.00	75.93	89.50	74.36
468	361.43	68.17	81.14	75.70	79.06	89.67	75.19
Average	332.20	64.41	80.17	67.78	79.29	86.35	73.36
Min	250.00	56.83	75.26	54.17	74.34	69.17	64.93
Max	398.39	80.84	84.25	87.83	83.06	106.96	80.76
Standard Dev	36.15	4.97	2.46	8.49	2.21	7.50	3.93

Phase 2 COD Removal ANOVA

COD Removal

@24°C	COD Removal @10°C	COD Removal @10°C
79.12	78.09110629	70.77006508
79.62	77.49318801	69.70027248
78.55	76.12716763	70.1734104
77.57	74.86842105	64.93421053
75.26	79.05798969	67.65463918
75.93	77.93333333	67
81.32	81.17138599	73.9195231
79.42	80.29609246	77.15905338
79.92	81.19097222	70.25347222
77.51	79.51246201	69.54407295
78.57	80.09137056	72.6463621
79.82	79.66085578	76.49128368
78.86	77.23238381	73.51424288
76.23	80.39491201	70.59383832
79.18	80.81895963	70.76237597
81.93	81.57053509	76.83669215
83.68	82.63845311	80.75503903
82.76	81.93880454	80.12828803
84.25	83.06429133	77.27714283
83.73	79.88796105	75.65508756
82.14	79.95143463	76.32298761
83.73	79.6261878	76.96395382
81.74	74.34272026	75.21909325
81.69	79.46624711	73.52906252
80.90	75.93399037	74.35823974
81.14	79.05541875	75.19021664

H0: $\mu_1 = \mu_2 = \mu_3$

Anova: Single Factor

SUMMARY

Groups	Count	Sum	Average	Variance
Column 1	26	2084.55	80.17	6.28
Column 2	26	2061.42	79.29	5.09
Column 3	26	1907.35	73.36	16.03

ANOVA

Source of Variation	SS	df	MS	F	P-value	F crit
Between Groups	713.7072666	2	356.85	39.07	0.00	3.12
Within Groups	685.0697447	75	9.13			
Total	1398.777011	77				

Pair (1,2) Mean Difference	0.889685225	SE(1,2)	0.592720691
Pair (1,3) Mean Difference	6.81522442	SE(1,3)	0.592720691
Pair (2,3) Mean Difference	5.925539195	SE(2,3)	0.592720691

q(24°C,10°C)	=	11.50
df	=	75
qCritical (from Studentized Range)	=	3.38
q(24°C,10°C) > qCritical	The difference between the two means is significant at a significance level of 0.05.	

q(24°C,10°C*)	=	1.50
df	=	75
qCritical (from Studentized Range)	=	3.38
q(24°C,10°C*) < qCritical	The difference between the two means is NOT significant at a significance level of 0.05.	

q(10°C*,10°C)	=	10.00
df	=	75
qCritical (from Studentized Range)	=	3.38
q(10°C*,10°C) > qCritical	The difference between the two means is significant at a significance level of 0.05.	

*Previously operated at 15°C in Phase 1

Phase 2 Methane Production Data

Day	Influent COD	24°C AnMBR	10°C AnMBR	10°C AnMBR
313	341.50	116.04	64.43	22.45
317	364.30	122.61	66.24	21.50
321	305.34	110.88	67.34	31.82
324	317.17	123.55	56.30	31.68
328	312.83	124.20	61.82	30.58
331	341.50	123.65	68.54	35.90
334	341.50	116.47	66.82	34.12
337	323.48	109.30	62.38	29.38
342	315.99	107.18	64.94	31.68
345	307.51	107.71	66.24	31.68
349	336.89	92.93	53.38	31.68
352	318.55	126.96	44.16	26.40
356	349.91	116.28	51.74	19.22
359	345.60	111.31	68.54	16.85
363	355.22	115.59	61.82	16.80
372	331.50	116.28	64.51	16.42
377	321.20	111.89	73.97	13.04
380	337.34	101.23	62.38	12.67
384	377.34	97.20	52.27	12.29
387	288.33	95.88	64.51	13.63
391	253.33	108.00	59.62	14.59
394	258.67	107.52	56.45	11.90
399	250.00	101.76	54.43	14.59
402	335.50	109.44	51.91	16.70
405	302.83	110.35	50.40	15.74
408	288.00	119.45	50.40	23.52
412	274.17	96.00	58.46	29.90
415	295.50	106.08	57.46	26.54
419	315.50	108.72	58.56	29.88
422	333.50	101.12	53.57	32.26
426	340.06	92.16	50.18	37.63
429	365.83	96.96	42.12	35.71
433	359.75	101.69	46.80	34.18
436	398.39	120.96	44.62	34.20
440	386.63	105.60	42.12	37.34
443	394.61	110.40	41.50	38.45
447	382.01	96.48	41.18	39.40
450	358.28	91.20	41.50	38.40
454	382.01	91.20	38.06	37.40
457	342.32	96.00	37.44	35.40
461	336.86	100.80	36.50	34.50
464	349.04	91.20	36.19	36.20
468	361.43	96.00	35.88	35.90
Average	332.49	102.05	48.64	28.04
Min	250.00	91.20	35.88	11.90
Max	398.39	120.96	64.51	39.40
Standard Dev	35.83	8.03	8.66	10.02

Phase 2 VFA Data

Day	Influent VFA	24°C AnMBR	10°C AnMBR	10°C AnMBR w PAC
310	7.77	0.00	0.00	3.57
313	0.55	0.00	0.00	4.57
317	10.36	0.00	0.00	5.68
321	11.36	0.00	0.00	6.32
324	12.44	0.00	0.00	6.78
328	10.94	0.00	0.00	7.01
331	14.47	0.00	0.00	7.24
334	15.24	0.00	0.00	7.32
337	12.44	0.00	0.00	7.35
342	10.85	0.00	0.00	8.42
345	11.44	0.00	0.00	8.05
349	13.46	0.00	0.00	6.44
352	11.34	0.00	0.00	5.77
356	10.10	0.00	0.00	6.43
359	10.35	0.00	0.00	7.66
363	3.55	0.00	0.00	8.35
367	5.79	0.00	0.00	8.34
372	10.33	0.00	0.00	8.43
377	13.44	2.14	0.00	7.98
380	20.44	0.00	1.09	5.47
384	11.46	0.00	1.28	6.72
387	10.47	0.00	1.24	9.55
391	12.44	0.00	0.96	9.33
394	14.43	0.00	2.56	9.35
399	16.43	0.00	2.38	8.37
402	13.59	0.00	2.34	5.54
405	14.44	0.00	2.90	6.23
408	16.23	0.00	3.57	6.24
412	10.99	0.00	4.22	7.54
415	11.23	0.00	3.59	5.24
419	11.35	0.00	3.99	5.54
422	10.55	0.00	4.98	7.21
426	13.08	0.00	5.88	8.26
429	14.43	0.00	6.76	9.12
433	12.44	0.00	5.92	9.03
436	16.43	0.00	6.77	8.55
440	13.55	1.35	7.22	7.35
443	11.35	0.00	8.44	8.54
447	10.55	0.00	6.77	9.13
450	4.26	0.00	7.10	9.37
454	10.44	0.00	7.09	5.23
457	12.46	0.00	7.21	10.36
461	0.67	0.00	7.46	9.54
464	12.46	0.00	7.36	8.35
468	11.06	0.00	4.09	8.63
Average	11.41	0.05	4.74	7.84
Min	0.55	0.00	0.96	5.23
Max	20.44	1.35	8.44	10.36
Standard Dev	3.75	0.26	2.33	1.56

Appendix C – Phase 3 Data for All AnMBRs

Phase 3 COD Data

Day	Influent COD	Effluent COD @24°C		Effluent COD @10°C		COD Rem @10°C		Effluent COD		COD Rem	
		@24°C	COD Rem @24°C	w/ NO PAC	NO PAC	@10°C w/ PAC	@10°C PAC				
468	361.43	68.17	81.14	84.00	76.76	88.83	75.42				
471	379.59	74.50	80.37	83.67	77.96	84.50	77.74				
476	345.76	80.33	76.77	88.17	74.50	87.17	74.79				
479	359.40	83.33	76.81	88.83	75.28	83.17	76.86				
482	346.88	89.00	74.34	93.50	73.05	103.50	70.16				
484	356.23	90.67	74.55	93.17	73.85	107.33	69.87				
486	392.49	92.00	76.56	100.50	74.39	105.17	73.21				
489	393.99	103.83	73.65	101.17	74.32	103.50	73.73				
492	381.84	105.83	72.28	109.33	71.37	108.50	71.58				
496	386.14	109.00	71.77	106.83	72.33	103.50	73.20				
499	377.16	111.50	70.44	109.83	70.88	104.17	72.38				
503	402.96	99.00	75.43	93.50	76.80	103.50	74.32				
507	408.57	90.50	77.85	108.00	73.57	98.50	75.89				
510	416.23	91.00	78.14	108.00	74.05	93.83	77.46				
513	414.74	90.50	78.18	110.17	73.44	93.67	77.42				
517	423.52	101.33	76.07	107.33	74.66	92.00	78.28				
521	425.39	101.33	76.18	125.17	70.58	95.17	77.63				
524	412.87	100.50	75.66	124.50	69.84	91.17	77.92				
527	413.24	107.67	73.95	129.33	68.70	103.50	74.95				
531	407.07	107.83	73.51	130.33	67.98	99.83	75.48				
534	418.29	118.50	71.67	128.50	69.28	103.50	75.26				
538	421.37	109.69	73.97	137.83	67.29	105.33	75.00				
541	418.02	113.04	72.96	156.67	62.52	109.00	73.92				
545	427.66	115.34	73.03	150.83	64.73	107.50	74.86				
548	442.32	121.63	72.50	156.83	64.54	114.17	74.19				
552	433.52	119.32	72.48	152.50	64.82	117.17	72.97				
555	492.80	125.60	74.51	158.17	67.90	123.33	74.97				
559	473.53	119.53	74.76	160.33	66.14	121.83	74.27				
562	454.47	121.00	73.38	167.92	63.05	124.50	72.61				
565	462.64	125.19	72.94	144.04	68.87	123.00	73.41				
568	463.47	121.00	73.89	161.63	65.13	116.60	74.84				
572	436.45	125.19	71.32	155.14	64.45	121.21	72.23				
576	413.20	124.77	69.80	145.92	64.68	123.51	70.11				
Average	411.01	104.78	74.57	123.38	70.23	104.88	74.45				
Min	345.76	68.17	69.80	83.67	62.52	83.17	69.87				
Max	492.80	125.60	81.14	167.92	77.96	124.50	78.28				
Standard Dev	35.57	15.55	2.62	26.37	4.40	11.81	2.23				

Phase 3 COD Removal ANOVA

Day	COD Rem @24°C	COD Rem @10°C	COD Rem @10°C PAC
468	81.14	76.76	75.42
471	80.37	77.96	77.74
476	76.77	74.50	74.79
479	76.81	75.28	76.86
482	74.34	73.05	70.16
484	74.55	73.85	69.87
486	76.56	74.39	73.21
489	73.65	74.32	73.73
492	72.28	71.37	71.58
496	71.77	72.33	73.20
499	70.44	70.88	72.38
503	75.43	76.80	74.32
507	77.85	73.57	75.89
510	78.14	74.05	77.46
513	78.18	73.44	77.42
517	76.07	74.66	78.28
521	76.18	70.58	77.63
524	75.66	69.84	77.92
527	73.95	68.70	74.95
531	73.51	67.98	75.48
534	71.67	69.28	75.26
538	73.97	67.29	75.00
541	72.96	62.52	73.92
545	73.03	64.73	74.86
548	72.50	64.54	74.19
552	72.48	64.82	72.97
555	74.51	67.90	74.97
559	74.76	66.14	74.27
562	73.38	63.05	72.61
565	72.94	68.87	73.41
568	73.89	65.13	74.84
572	71.32	64.45	72.23
576	69.80	64.68	70.11

Anova: Single Factor

SUMMARY

Groups	Count	Sum	Average	Variance
Column 1	33	2460.85	74.57	7.09
Column 2	33	2317.72	70.23	20.01
Column 3	33	2456.92	74.45	5.11

ANOVA

Source of Variation	SS	df	MS	F	P-value	F crit
Between Groups	402.85	2	201.42	18.76	0.00	3.09
Within Groups	1030.52	96	10.73			
Total	1433.36	98				

Pair (1,2) Mean Difference	4.3374927	SE(1,2)	0.570342
Pair (1,3) Mean Difference	0.1191472	SE(1,3)	0.570342
Pair (2,3) Mean Difference	4.2183455	SE(2,3)	0.570342

q(24°C, 10°C PAC)	=	0.21
df	=	96
qCritical (from Studentized Range)	=	3.37
q(24°C, 10°C PAC) < qCritical	The difference between the two means is NOT significant at a significance level of 0.05.	

q(24°C, 10°C NO PAC)	=	0.40
df	=	96
qCritical (from Studentized Range)	=	3.37
q(24°C, 10°C NO PAC) < qCritical	The difference between the two means is NOT significant at a significance level of 0.05.	

q(10°C NO PAC, 10°C PAC)	=	0.39
df	=	96
qCritical (from Studentized Range)	=	3.37
q(10°C NO PAC, 10°C PAC) < qCritical	The difference between the two means is NOT significant at a significance level of 0.05.	

Phase 3 Methane Production Data

Day	Influent COD	24°C AnMBR	CH4-COD (mg/L)	10°C AnMBR w/ NO PAC	CH4-COD (mg/L)	10°C AnMBR w/ PAC	CH4-COD (mg/L)
468	361.43	96	274.29	35.88	102.51	38.466	109.90
471	379.59	105.6	301.71	35.88	102.51	36.77	105.06
476	345.76	110.88	316.80	37.44	106.97	36.4	104.00
479	359.40	116.16	331.89	37.44	106.97	36.7	104.86
482	346.88	105.6	301.71	38.376	109.65	37.89	108.26
484	356.23	104.88	299.66	52.416	149.76	39.56	113.03
486	392.49	113.712	324.89	53.2224	152.06	48.4	138.29
489	393.99	126.96	362.74	54.432	155.52	56.7	162.00
492	381.84	126.96	362.74	53.76	153.60	57.88	165.37
496	386.14	132.48	378.51	63.84	182.40	62.14	177.54
499	377.16	121.44	346.97	57.12	163.20	63.44	181.26
503	402.96	115.92	331.20	57.6	164.57	66.43	189.80
507	408.57	147.84	422.40	60.48	172.80	64.56	184.46
510	416.23	137.28	392.23	63.84	182.40	65.33	186.66
513	414.74	153.12	437.49	82.08	234.51	85.56	244.46
517	423.52	154.56	441.60	103.68	296.23	100.43	286.94
521	425.39	160.08	457.37	104.88	299.66	102.34	292.40
524	412.87	165.6	473.14	100.32	286.63	110.34	315.26
527	413.24	171.12	488.91	95.76	273.60	118.8	339.43
531	407.07	165.6	473.14	110.88	316.80	122.4	349.71
534	418.29	154.56	441.60	115.92	331.20	114.24	326.40
538	421.37	165.6	473.14	110.88	316.80	122.4	349.71
541	418.02	165.6	473.14	110.4	315.43	134.64	384.69
545	427.66	165.6	473.14	114.048	325.85	133.55	381.57
548	442.32	171.12	488.91	111.744	319.27	134.32	383.77
552	433.52	162	462.86	112.2	320.57	134.52	384.34
555	492.80	161.28	460.80	133.728	382.08	135.66	387.60
559	473.53	156	445.71	119.616	341.76	134.5	384.29

562	454.47	168	480.00	123.648	353.28	133.45	381.29
565	462.64	174	497.14	122.304	349.44	140.33	400.94
568	463.47	150	428.57	128.88	368.23	141.984	405.67
572	436.45	162	462.86	118.8	339.43	135.55	387.29
576	413.20	156	445.71	123.84	353.83	133.22	380.63
Average	411.01	160.96	459.87	110.37	315.35	121.68	347.65
Min	345.76	137.28	392.23	63.84	182.40	65.33	186.66
Max	492.80	174.00	497.14	133.73	382.08	141.98	405.67
Standard Dev	35.57	8.40	23.99	15.73	44.95	19.64	56.12

Phase 3 VFA Data

Day	Influent	24°C AnMBR	10°C AnMBR w/ NO PAC	10°C AnMBR w/ PAC
468	11.06	0.00	9.11	8.63
471	12.51	0.00	7.91	7.43
476	15.33	0.00	7.91	6.74
479	21.09	0.00	10.07	9.73
482	18.21	0.00	7.86	8.46
484	16.15	0.00	7.023	6.03
486	11.70	0.00	13.50	12.89
489	15.11	0.00	11.03	12.47
492	19.35	0.00	14.51	13.79
496	16.88	0.00	11.98	11.49
499	17.03	0.00	7.79	6.13
503	18.65	0.00	11.12	8.96
507	17.21	0.00	12.02	8.60
510	17.28	0.00	14.69	10.51
513	15.25	0.00	12.96	9.27
517	19.78	0.00	15.88	10.14
521	20.97	0.00	17.85	11.39
524	27.73	0.00	22.01	16.12
527	20.97	0.00	17.85	11.39
531	17.63	0.00	19.25	12.68
534	14.33	0.00	17.19	12.13
538	14.77	0.00	18.81	12.18
541	22.51	1.87	20.74	10.20
545	17.70	0.00	22.14	8.66
548	24.74	0.00	27.66	7.30
552	15.30	0.00	22.33	6.80
555	31.90	0.00	36.65	8.99
559	18.23	0.00	36.95	6.30
562	12.65	1.14	12.823	8.20
565	15.78	0.00	22.00	8.90
568	15.09	0.00	20.21	7.30
572	19.00	0.00	38.53	7.50
576	17.98	1.06	9.99	6.78
Average	17.87	0.20	21.32	9.64
Min	11.06	0.00	9.99	6.30
Max	31.90	1.87	38.53	16.12
Standard Dev	4.29	0.50	7.80	2.43